

Correlated interaction effects in three-dimensional semi-Dirac semimetal

Jing-Rong Wang,¹ Wei Li,^{2,*} and Chang-Jin Zhang^{1,3,†}

¹*High Magnetic Field Laboratory of Anhui Province,
Anhui Province Key Laboratory of Condensed Matter Physics at Extreme Conditions,
Chinese Academy of Sciences, Hefei 230031, China*

²*Key Laboratory of Materials Physics, Institute of Solid State Physics,
Chinese Academy of Sciences, Hefei 230031, China*

³*Institute of Physical Science and Information Technology, Anhui University, Hefei 230601, China*

Understanding the correlation effects in unconventional topological materials, in which the fermion excitations take unusual dispersion, is an important topic in recent condensed matter physics. We study the influence of short-range four-fermion interactions on three-dimensional semi-Dirac semimetal with an unusual fermion dispersion, that is linear along two directions but quadratic along the third one. Based on renormalization group theory, we find all of 11 unstable fixed points including 5 quantum critical points, 5 bicritical points, and one tricritical point. The physical essences of the quantum critical points are determined by analyzing the susceptibility exponents for all of the source terms in particle-hole and particle-particle channels. We also verify phase diagram of the system in the parameter space carefully through numerically studying the flows of the four-fermion coupling parameters and behaviors of the susceptibility exponents. These results are helpful for us to understand the physical properties of candidate materials for three-dimensional semi-Dirac semimetal such as ZrTe₅.

I. INTRODUCTION

The past 15 years have witnessed that study about topological materials becomes one of the most important fields in condensed matter physics [1–9]. Topological materials have wide potential implications as electronic devices due to their some fascinating physical properties. In some topological materials, such as Dirac semimetal (DSM) including Cd₃As₂ and Na₃Bi, and Weyl semimetal (WSM) including TaAs, TaP, NbAs, and NbP, the low-energy fermion excitations are Dirac fermions or Weyl fermions which resemble the elementary particles in high energy physics. Thus, these materials provide a platform to verify some important concepts in high energy physics.

Besides Dirac and Weyl fermions, there could be unconventional fermions with unusual dispersion in topological materials. In double- (triple-) WSM, the fermion dispersion is quadratic (cubic) along two directions but linear along the third one [11, 12]. At the topological quantum critical point (QCP) between DSM or WSM and band insulator, the fermion dispersion is mixture of linear and quadratic ones [13, 14]. Higher spin fermions with multiband crossing have also attracted a lot of interest recently [15–17]. Spin-1 chiral fermions characterized by combination of a Dirac-like band and a flat band with three-bands crossing, and spin-3/2 chiral fermions displaying a birefringent spectrum with two distinct Fermi velocities have been observed recently [18–22].

The correlation effects in Dirac and Weyl fermion systems are extensively studied, and are well understood

relatively [23–34]. The influence of many-body interaction on unconventional fermion systems also attracted much interest and is an important topic. There have been studies about influence of long-range Coulomb interaction [37–51], short-range four-fermion interaction [52–56], and quantum fluctuation of order parameter [57–60] on some unconventional fermion systems. These studies revealed many novel behaviors, such as various quantum phase transitions, non-Fermi liquid behaviors, anisotropic screening effect *etc.* These studies also showed that the correlation effects in unconventional fermion systems depend on the fermion dispersion subtly.

However, there are still a lot of open questions about the correlation effects in unconventional fermion systems. In this article, we pay attention to the influence of short-range four-fermion interactions on three-dimensional (3D) semi-DSM, in which the fermion dispersion is linear along two directions but quadratic along the third one as shown in Fig. 1. 3D semi-DSM state could be realized at the topological QCP between 3D DSM and band insulator [14].

The rest of paper is structured as follows. The model is defined in Sec. II. In Sec. III, we show the results based on renormalization group (RG) theory. The results are summarized and some discussion is given in Sec. IV. The detailed derivation of the RG equations and susceptibility exponents for the source terms and careful numerical analysis are presented in Appendices.

II. MODEL

The free action for 3D semi-DSM can be written as

$$S_0 = \int \frac{d\omega}{2\pi} \frac{d^3\mathbf{k}}{(2\pi)^3} \bar{\Psi}(\omega, \mathbf{k}) [i\omega\gamma_0 + \mathcal{H}(\mathbf{k})] \Psi(\omega, \mathbf{k}), \quad (1)$$

*Corresponding author: wliustc@theory.issp.ac.cn

†Corresponding author: zhangcj@hmf.ac.cn

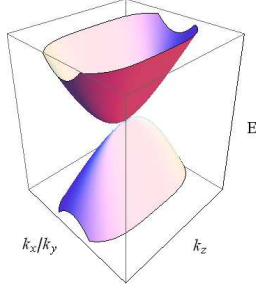


FIG. 1: Energy dispersion of fermions in 3D semi-DSM.

where the Hamiltonian density $\mathcal{H}(\mathbf{k})$ is given by

$$\mathcal{H}(\mathbf{k}) = iv\gamma_1 k_1 + ivk_2\gamma_2 + iAk_3^2\gamma_3, \quad (2)$$

with v and A being model parameters. Ψ is four component spinor, and $\bar{\Psi} = \Psi^\dagger\gamma_0$. The gamma matrices are defined as $\gamma_0 = \tau_2 \otimes \sigma_0$, $\gamma_1 = \tau_3 \otimes \sigma_1$, $\gamma_2 = \tau_3 \otimes \sigma_2$, $\gamma_3 = \tau_3 \otimes \sigma_3$, and $\gamma_5 = \tau_1 \otimes \sigma_0$, where $\tau_{1,2,3}$ and $\sigma_{1,2,3}$ are Pauli matrices. The gamma matrices satisfy the anticommutation relation $\{\gamma_\mu, \gamma_\nu\} = 2\delta_{\mu\nu}$ for $\mu, \nu = 0, 1, 2, 3, 5$. The energy dispersion of fermions takes the form $E(\mathbf{k}) = \pm\sqrt{v^2k_\perp^2 + A^2k_3^4}$ where $k_\perp^2 = k_1^2 + k_2^2$. Density of states (DOS) is given by $\rho(\omega) \propto \omega^{3/2}/(v\sqrt{A})$, which vanishes at the Fermi level.

Due to the vanishing DOS, the weak four-fermion interaction is irrelevant in 3D semi-DSM. However, if the four-fermion interaction is strong enough, the system could be driven to a new phase. As shown in the Appendices, there are formally 12 kinds of four-fermion interactions. Whereas, due to the constraint by Fierz identity, five of them are linearly independent. Here, we consider the interacting Lagrangian as following

$$\begin{aligned} \mathcal{L}_{int} = & g_1 (\bar{\Psi}\gamma_0\Psi)^2 + g_2 (\bar{\Psi}\Psi)^2 + g_4 (\bar{\Psi}\gamma_0\gamma_5\Psi)^2 \\ & + g_5 (\bar{\Psi}i\gamma_5\Psi)^2 + g_{3z} (\bar{\Psi}\gamma_0\gamma_3\Psi)^2. \end{aligned} \quad (3)$$

In this article, we study the influence of four-fermion interactions on 3D semi-DSM through the RG method [61].

III. RG RESULTS

As shown in the Appendices, we firstly calculate all of the corrections from the one-loop Feynman diagrams, by employing a momentum shell $b\Lambda < \sqrt{v^2k_\perp^2 + A^2k_3^4} < \Lambda$, where $b = e^{-\ell}$ with ℓ being the RG running parameter. Then, we consider these corrections, and perform RG transformations to restore the original form of the actions. Accordingly, we obtain the RG equations for g_a , which can be formally written as

$$\frac{dg_a}{d\ell} = -\frac{3}{2}g_a + F_a(g_1, g_2, g_4, g_5, g_{3z}), \quad (4)$$

where $a = 1, 2, 4, 5, 3z$, The concrete expressions of F_a can be found in the Appendices.

TABLE I: There are 5 QCPs among the 11 non-trivial unstable fixed points. The corresponding order parameters for the five QCPs are shown in second rows.

	FP1	FP2	FP3	FP4	FP5
Order parameter	Δ_2	Δ_5	Δ_2/Δ_5	Δ_{7z}	Δ_{8z}

Solving the equations

$$\left. \frac{dg_a}{d\ell} \right|_{(g_1, g_2, g_4, g_5, g_{3z}) = (g_1^*, g_2^*, g_4^*, g_5^*, g_{3z}^*)} = 0, \quad (5)$$

we get 12 fixed points, including the trivial Gauss fixed point $(g_1^*, g_2^*, g_4^*, g_5^*, g_{3z}^*) = (0, 0, 0, 0, 0)$ and 11 non-trivial fixed points

$$\text{FP}i : (g_1^*, g_2^*, g_4^*, g_5^*, g_{3z}^*) = (g_{1,i}^*, g_{2,i}^*, g_{4,i}^*, g_{5,i}^*, g_{3z,i}^*), \quad (6)$$

with $i = 1, 2, \dots, 11$.

Expanding the RG equations of g_a in the vicinity of a fixed point, we obtain

$$\frac{d\delta g_a}{d\ell} = \sum_b M_{ab} \delta g_b, \quad (7)$$

where $\delta g_a = g_a - g_a^*$. M is five dimension square matrix, and the matrix elements are expressions of $g_1^*, g_2^*, g_4^*, g_5^*, g_{3z}^*$. From eigenvalues of M at a fixed point $(g_1^*, g_2^*, g_4^*, g_5^*, g_{3z}^*)$, we can get the properties of the fixed point. A negative (positive) eigenvalue is corresponding to a stable (unstable) eigendirection [32, 34]. There is one unstable direction for QCP, and there are two and three unstable directions for bicritical point (BCP) and tricritical point (TCP) respectively. Substituting the values of g_a^* at each fixed point into the expression of M , we calculate the corresponding eigenvalues of M . We find that FP1, FP2, FP3, FP4, and FP5 are QCPs, FP6, FP7, FP8, FP9, and FP10 are BCPs, and FP11 is a TCP.

For a QCP, the correlation length exponent ν is determined by the inverse of the corresponding positive eigenvalue of M . For the five QCPs, ν always satisfies

$$\nu^{-1} = 1.5. \quad (8)$$

In order to determine the physical essences of the QCPs, we analyze the RG flows of all the fermion bilinear source terms in particle-hole and particle-particle channels. The source terms in particle-hole channel can be generally written as

$$S_s = \Delta_X \int \frac{d\omega}{2\pi} \frac{d^3\mathbf{k}}{(2\pi)^3} \bar{\Psi}(\omega, \mathbf{k}) \Gamma_X \Psi(\omega, \mathbf{k}). \quad (9)$$

There are 12 choices for the matrix Γ_X , which corresponds to 12 different order parameters in particle-hole channel. The source terms in particle-particle channel take the general form

$$S_s = \Delta_Y \int \frac{d\omega}{2\pi} \frac{d^3\mathbf{k}}{(2\pi)^3} \Psi^\dagger(\omega, \mathbf{k}) \Gamma_Y \Psi^*(\omega, \mathbf{k}). \quad (10)$$

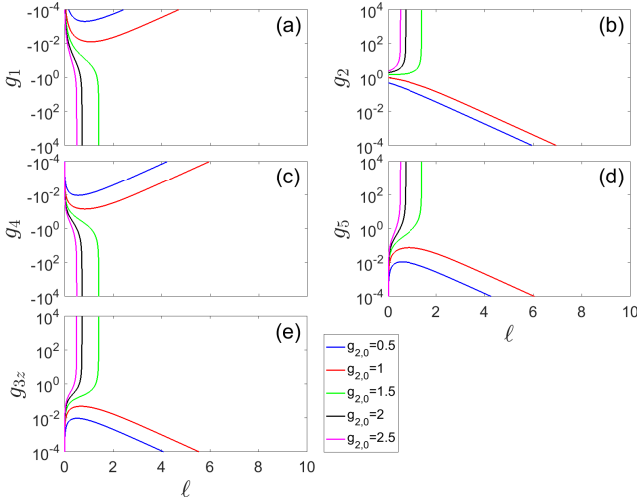


FIG. 2: (a)-(e): Flows of g_1 , g_2 , g_4 , g_5 , and g_{3z} with different initial conditions. $g_{1,0} = 0$, $g_{4,0} = 0$, $g_{5,0} = 0$, and $g_{3z,0} = 0$ are taken.

There are 6 choices for the matrix Γ_Y , which is corresponding to 6 different superconducting pairings.

Firstly, we calculate the one-loop order corrections to the source terms as shown in Eqs. (9) and (10) induced by the four-fermion interactions as shown in Eq. (3). Then, we include these corrections and perform RG transformations to restore the original form of the source terms. Accordingly, through the RG transformations, we obtain the equations

$$\bar{\beta}_{X,Y} = H_{X,Y}(g_1, g_2, g_4, g_5, g_{3z}), \quad (11)$$

where

$$\bar{\beta}_{X,Y} = \frac{d \ln(\Delta_{X,Y})}{d\ell} - 1. \quad (12)$$

$\bar{\beta}_{X,Y}$ is usually termed as susceptibility exponent or anomalous dimension for the fermion-bilinear source term. $H_{X,Y}$ are functions of g_a with $a = 1, 2, 4, 5, 3z$. The concrete expressions of $H_{X,Y}$ are shown in Appendices. For a QCP, substituting the values of g_a at the QCP into Eq. (11), and finding the largest one among all of $\bar{\beta}_{X,Y}$, we can determine the physical meaning of the QCP.

For FP1, $\bar{\beta}_2$ takes the largest value. It represents that this fixed point is corresponding to the QCP to a state in which the order parameter $\Delta_2 = \langle \bar{\Psi} \Psi \rangle$ acquires finite value. The physical meaning of Δ_2 is scalar mass.

For FP2, $\bar{\beta}_5$ is the largest one. It means that this fixed point stands for the QCP to a state in which the order parameter $\Delta_5 = \langle \bar{\Psi} i\gamma_5 \Psi \rangle$ becomes finite. The physical meaning of Δ_5 corresponds to pseudoscalar mass.

For FP3, $\bar{\beta}_2$ and $\bar{\beta}_5$ are largest simultaneously. It indicates that the fixed point corresponds to the QCP to a phase in which both of Δ_2 and Δ_5 become finite. The parameter of this phase can be written as

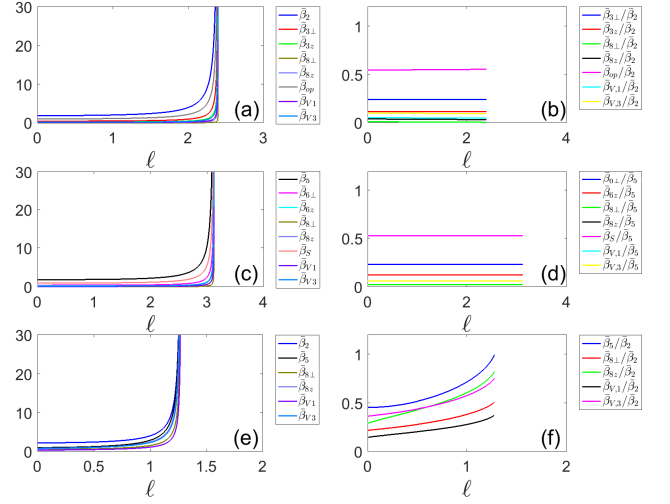


FIG. 3: Flows of $\bar{\beta}_{X,Y}$ which approach positive infinity and ratios between $\bar{\beta}_{X,Y}$. (a) and (b): $g_{1,0} = 0.15$, $g_{2,0} = 1.3$, $g_{4,0} = 0.46$, $g_{5,0} = -0.56$, and $g_{3z,0} = 0.055$ are taken; (c) and (d): $g_{2,0} = 0.14$, $g_{2,0} = -0.59$, $g_{4,0} = 0.42$, $g_{5,0} = 1.36$, and $g_{3z,0} = 0.07$ are taken; (e) and (f): $g_{1,0} = 1.5$, $g_{2,0} = 0$, $g_{3,0} = 0$, $g_{5,0} = 0.2$, and $g_{3z,0} = 0$ are taken.

$\langle \bar{\Psi} (\cos(\theta) + i\gamma_5 \sin(\theta)) \Psi \rangle$. This phase represents an axionic insulator [33].

For FP4, $\bar{\beta}_{7z}$ takes the largest value. It signifies that this fixed point is corresponding to the QCP to a state in which the order parameter $\Delta_{7z} = \langle \bar{\Psi} i\gamma_5 \gamma_3 \Psi \rangle$ becomes finite. Δ_{7z} stands for axial magnetization along z axis.

For FP5, $\bar{\beta}_{8z}$ is the largest one. It suggests that this fixed point represents the QCP to a state with finite order parameter $\Delta_{8z} = \langle \bar{\Psi} i\gamma_3 \Psi \rangle$. The physical meaning of Δ_{8z} is current along z axis.

For convenience, we summarize the corresponding order parameters for the 5 QCPs in Table I.

For general given initial conditions that is decided by $(g_{1,0}, g_{2,0}, g_{4,0}, g_{5,0}, g_{3z,0})$, we determine the corresponding phase through the flows of four-fermion coupling parameters g_a and flows of susceptibility exponents $\beta_{X,Y}$. We show the flows of g_1 , g_2 , g_4 , g_5 , and g_{3z} under several initial conditions in Fig. 2. If g_a with $a = 1, 2, 4, 5, 3z$ approach to zero, it represents that the system is still in SM phase. If $|g_a|$ with $a = 1, 2, 4, 5, 3z$ flow to infinity at a finite running parameter ℓ_c , the system becomes unstable to a new phase.

In order to determine the physical essence of the new phase, we calculate the flows of the susceptibility exponents $\bar{\beta}_{X,Y}$ and compare them. For three general initial conditions, the flows of $\bar{\beta}_{X,Y}$ and the ratio between them are presented in Figs. 3(a)-3(f). Here we only show the susceptibility exponents that approach to positive infinity in Figs. 3(a), 3(c), and 3(e) respectively. For the initial condition corresponding to Figs. 3(a) and 3(b), we can find that $\bar{\beta}_2$ approaches to positive infinity most quickly. It means that scalar mass Δ_2 is generated in the new phase. For the initial condition corresponding

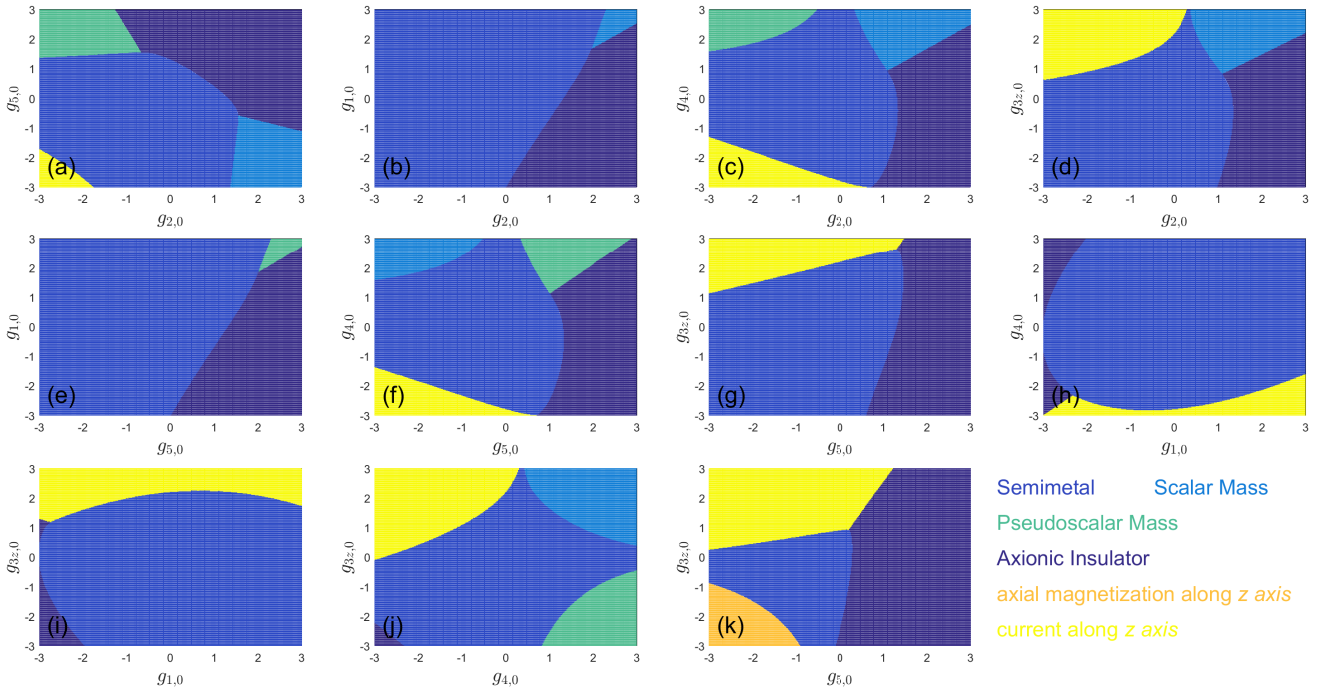


FIG. 4: Phase diagrams on the planes of two initial values of four-fermion coupling strength. (a) $g_{2,0}$ and $g_{5,0}$; (b) $g_{2,0}$ and $g_{1,0}$; (c) $g_{2,0}$ and $g_{4,0}$; (d) $g_{2,0}$ and $g_{3z,0}$; (e) $g_{5,0}$ and $g_{1,0}$; (f) $g_{5,0}$ and $g_{4,0}$; (g) $g_{5,0}$ and $g_{3z,0}$; (h) $g_{1,0}$ and $g_{4,0}$; (i) $g_{1,0}$ and $g_{3z,0}$; (j) $g_{4,0}$ and $g_{3z,0}$; (k) $g_{5,0}$ and $g_{3z,0}$. In (a)-(j), the initial values of rest four-fermion coupling parameters are taken as zero. For example, $g_{1,0} = 0$, $g_{4,0} = 0$ and $g_{3z,0} = 0$ are taken in (a). In (k), $g_{1,0} = -2.3$, $g_{2,0} = 0$, and $g_{4,0} = -0.62$ are taken.

to Figs. 3(c) and 3(d), $\bar{\beta}_5$ flows to positive infinity with the largest speed. It indicates that pseudoscalar mass Δ_5 becomes finite in the new phase. For the initial condition corresponding to Figs. 3(e) and 3(f), we can find that $\bar{\beta}_2$ and $\bar{\beta}_5$ approach to positive infinity most quickly and $\bar{\beta}_5/\bar{\beta}_2 \rightarrow 1$. It represents that the system becomes to a new phase that Δ_2 and Δ_5 acquire finite value simultaneously. Namely, the system becomes to axionic insulating phase.

The phase diagrams on the planes composed by initial values of two four-fermion coupling parameters are shown in Fig. 4. Different phases are marked by different colors. In Figs. 4(a)-4(j), we show all the 10 phase diagrams on the planes composed by initial values of two coupling parameters chosen from the five linearly independent coupling parameters. The initial values of rest of three coupling parameters are taken as zero. Taken Fig. 4(a) composed by $g_{2,0}$ and $g_{5,0}$ as an example, we can notice that there are five phases, SM, insulator with scalar mass Δ_2 , insulator characterized by pseudoscalar mass Δ_5 , axionic insulating phase, and a phase with current along z axis Δ_{8z} . In Fig. 4(k), we present the phase diagram composed by $g_{5,0}$ and $g_{3z,0}$. In this phase diagram, $g_{1,0}$, $g_{2,0}$ and $g_{4,0}$ are taken as proper values so that the phase with axial magnetization along z axis Δ_{7z} appears in the phase diagram.

Recently, Sur and Roy studied the quantum critical behaviors in the vicinity of possible QCPs in various SMs with different dispersions generally [59]. Accord-

ing to their studies, in 3D semi-DSM, the Yukawa coupling between quantum fluctuation of order parameter and fermion excitations becomes irrelevant in the low energy regime. Thus, the fermions should take Fermi liquid behaviors in the vicinity of a QCP between SM phase and a symmetry breaking phase in 3D semi-DSM. Concretely, the residue of fermions Z_f approaches to a finite constant value in the lowest energy limit, and the Landau damping rate of fermions $\Gamma(\omega)$ satisfies

$$\lim_{\omega \rightarrow 0} \frac{\Gamma(\omega)}{\omega} \rightarrow 0. \quad (13)$$

Additionally, under the influence of quantum fluctuation of order parameter, the observable quantities DOS ρ , specific heat C_v , compressibility κ , optical conductivities within the xy and along z axis $\sigma_{\perp\perp}$ and σ_{zz} should respectively still take the behaviors

$$\begin{aligned} \rho(\omega) &\sim \omega^{3/2}, & C_v(T) &\sim T^{5/2}, & \kappa(T) &\sim T^{3/2}, \\ \sigma_{\perp\perp}(\omega) &\sim \omega^{1/2}, & \sigma_{zz}(\omega) &\sim \omega^{3/2}, \end{aligned} \quad (14)$$

which are qualitatively same as the ones for free fermions.

IV. SUMMARY

In summary, we perform comprehensive studies about the influence of four-fermion interactions on 3D semi-DSM through RG theory. We find 11 unstable fixed

points and show that five fixed points are QCPs, five fixed points are BCPs, and the rest one is a TCP. The physical essence of the QCPs are determined carefully by analyzing the scalings of fermion bilinear source terms. The phase diagrams for general initial conditions are also presented through detailed numerical calculations of flows of four-fermion couplings and susceptibility exponents.

According to the theoretical study by Yang and Nagaosa [14], 3D semi-DSM state can be realized at the topological QCP between 3D DSM and band insulator. Through magneto-optics and magneto-transport, Yuan *et al.* observed the evidence of 3D semi-DSM phase in ZrTe₅ [62]. The subsequent study about magnetotransport properties of ZrTe₅ under hydrostatic pressure also supports the existence of 3D semi-DSM phase [63]. Recent measurements of optical spectroscopy in ZrTe₅ are also consistent with 3D semi-DSM phase [64, 65]. 3D semi-DSM state was also realized in pressed Cd₃As₂ [66].

We expect our theoretical results are helpful for understanding the physical properties of these candidate materials of 3D semi-DSM.

ACKNOWLEDGEMENTS

J.R.W. is grateful to Prof. G.-Z. Liu for the valuable discussions. We acknowledge the support from the National Key R&D Program of China under Grants 2016YFA0300404, the National Natural Science Foundation of China under Grants 11974356, and U1832209, and the Collaborative Innovation Program of Hefei Science Center CAS under Grant 2019HSC-CIP002. A portion of this work was supported by the High Magnetic Field Laboratory of Anhui Province under Grant AHHM-FX-2020-01.

Appendix A: Fierz Identity

1. Fierz identity for 3D DSM

For 3D DSM, the interacting Lagrangian density can be written as [33]

$$\begin{aligned} \mathcal{L}_{\text{int}} = & g_1 (\bar{\Psi}\gamma_0\Psi)^2 + g_2 (\bar{\Psi}\Psi)^2 + g_3 \sum_{j=1}^3 (\bar{\Psi}\gamma_0\gamma_j\Psi)^2 + g_4 (\bar{\Psi}\gamma_0\gamma_5\Psi)^2 + g_5 (\bar{\Psi}i\gamma_5\Psi)^2 + g_6 \sum_{\langle lk \rangle} (\bar{\Psi}i\gamma_l\gamma_k\Psi)^2 \\ & + g_7 \sum_{j=1}^3 (\bar{\Psi}i\gamma_5\gamma_j\Psi)^2 + g_8 \sum_{j=1}^3 (\bar{\Psi}i\gamma_j\Psi)^2, \end{aligned} \quad (\text{A1})$$

where

$$\sum_{\langle lk \rangle} (\bar{\Psi}i\gamma_l\gamma_k\Psi)^2 = \left[(\bar{\Psi}i\gamma_2\gamma_3\Psi)^2 + (\bar{\Psi}i\gamma_3\gamma_1\Psi)^2 + (\bar{\Psi}i\gamma_1\gamma_2\Psi)^2 \right]. \quad (\text{A2})$$

There are eight kinds of four-fermion couplings. However, not all of them are linearly independent, due to the constraint by Fierz identity [31, 33, 34].

The Fierz identity indicates that [31, 33, 34]

$$[\bar{\Psi}(x)M\Psi(x)] [\bar{\Psi}(y)N\Psi(y)] = -\frac{1}{16} \text{Tr} [M\Gamma_a N\Gamma_b] [\bar{\Psi}(x)\Gamma_a\Psi(y)] [\bar{\Psi}(y)\Gamma_b\Psi(x)]. \quad (\text{A3})$$

For local interaction, we have $x = y$. Thus,

$$[\bar{\Psi}(x)M\Psi(x)] [\bar{\Psi}(x)N\Psi(x)] = -\frac{1}{16} \text{Tr} [M\Gamma_a N\Gamma_b] [\bar{\Psi}(x)\Gamma_a\Psi(x)] [\bar{\Psi}(x)\Gamma_b\Psi(x)]. \quad (\text{A4})$$

Repeat of indexes a and b in Eqs. (A3) and (A4) represents summation. Substituting each four-fermion coupling in Eq. (A1) into Eq. (A4), we could get eight equations, which can be compactly expressed by

$$FX = 0, \quad (\text{A5})$$

where

$$X = \begin{pmatrix} (\bar{\Psi}\gamma_0\Psi)^2 \\ (\bar{\Psi}\Psi)^2 \\ \sum_{j=1}^3 (\bar{\Psi}\gamma_0\gamma_j\Psi)^2 \\ (\bar{\Psi}\gamma_0\gamma_5\Psi)^2 \\ (\bar{\Psi}i\gamma_5\Psi)^2 \\ \sum_{\langle lk\rangle} (\bar{\Psi}i\gamma_l\gamma_k\Psi)^2 \\ \sum_{j=1}^3 (\bar{\Psi}i\gamma_5\gamma_j\Psi)^2 \\ \sum_{j=1}^3 (\bar{\Psi}i\gamma_j\Psi)^2 \end{pmatrix}, \quad (\text{A6})$$

and

$$F = \begin{pmatrix} 5 & 1 & 1 & 1 & 1 & 1 & 1 & 1 \\ 1 & 5 & -1 & -1 & -1 & 1 & 1 & -1 \\ 3 & -3 & 3 & -3 & 3 & 1 & -1 & 1 \\ 1 & -1 & -1 & 5 & -1 & -1 & 1 & 1 \\ 1 & -1 & 1 & -1 & 5 & -1 & 1 & -1 \\ 3 & 3 & 1 & -3 & -3 & 3 & -1 & 1 \\ 3 & 3 & -1 & 3 & 3 & -1 & 3 & -1 \\ 3 & -3 & 1 & 3 & -3 & 1 & -1 & 3 \end{pmatrix}. \quad (\text{A7})$$

It is easy to verify that rank of F is 4, namely

$$\text{Rank}(F) = 4. \quad (\text{A8})$$

Then, the number of linearly independent couplings is

$$8 - \text{Rank}(F) = 4. \quad (\text{A9})$$

For convenience, we take the four couplings

$$(\bar{\Psi}\gamma_0\Psi)^2, \quad (\bar{\Psi}\Psi)^2, \quad (\bar{\Psi}\gamma_0\gamma_5\Psi)^2, \quad (\bar{\Psi}i\gamma_5\Psi)^2, \quad (\text{A10})$$

as linearly independent couplings. The other couplings

$$\sum_{j=1}^3 (\bar{\Psi}\gamma_0\gamma_j\Psi)^2, \quad \sum_{\langle lk\rangle} (\bar{\Psi}i\gamma_l\gamma_k\Psi)^2, \quad \sum_{j=1}^3 (\bar{\Psi}i\gamma_5\gamma_j\Psi)^2, \quad \sum_{j=1}^3 (\bar{\Psi}i\gamma_j\Psi)^2, \quad (\text{A11})$$

can be expressed by the four independent couplings shown in Eq. (A10). In order to obtain the concrete expressions for other couplings, we define

$$\tilde{X} = \begin{pmatrix} \sum_{j=1}^3 (\bar{\Psi}\gamma_0\gamma_j\Psi)^2 \\ \sum_{\langle lk\rangle} (\bar{\Psi}i\gamma_l\gamma_k\Psi)^2 \\ \sum_{j=1}^3 (\bar{\Psi}i\gamma_5\gamma_j\Psi)^2 \\ \sum_{j=1}^3 (\bar{\Psi}i\gamma_j\Psi)^2 \\ (\bar{\Psi}\gamma_0\Psi)^2 \\ (\bar{\Psi}\Psi)^2 \\ (\bar{\Psi}\gamma_0\gamma_5\Psi)^2 \\ (\bar{\Psi}i\gamma_5\Psi)^2 \end{pmatrix}. \quad (\text{A12})$$

It is easy to find that

$$\tilde{F}\tilde{X} = 0, \quad (\text{A13})$$

where

$$\tilde{F} = \begin{pmatrix} 1 & 1 & 1 & 1 & 5 & 1 & 1 & 1 \\ -1 & 1 & 1 & -1 & 1 & 5 & -1 & -1 \\ 3 & 1 & -1 & 1 & 3 & -3 & -3 & 3 \\ -1 & -1 & 1 & 1 & 1 & -1 & 5 & -1 \\ 1 & -1 & 1 & -1 & 1 & -1 & -1 & 5 \\ 1 & 3 & -1 & 1 & 3 & 3 & -3 & -3 \\ -1 & -1 & 3 & -1 & 3 & 3 & 3 & 3 \\ 1 & 1 & -1 & 3 & 3 & -3 & 3 & -3 \end{pmatrix}. \quad (\text{A14})$$

Performing a series of similarity transformations for \tilde{F} ,

$$\tilde{F} \rightarrow \tilde{F}', \quad (\text{A15})$$

we obtain

$$\tilde{F}'\tilde{X} = 0, \quad (\text{A16})$$

where

$$\tilde{F}' = \begin{pmatrix} 1 & 0 & 0 & 0 & 1 & -1 & -1 & 2 \\ 0 & 1 & 0 & 0 & 1 & 2 & -1 & -1 \\ 0 & 0 & 1 & 0 & 2 & 1 & 1 & 1 \\ 0 & 0 & 0 & 1 & 1 & -1 & 2 & -1 \\ 0 & 0 & 0 & 0 & 0 & 0 & 0 & 0 \\ 0 & 0 & 0 & 0 & 0 & 0 & 0 & 0 \\ 0 & 0 & 0 & 0 & 0 & 0 & 0 & 0 \\ 0 & 0 & 0 & 0 & 0 & 0 & 0 & 0 \end{pmatrix}. \quad (\text{A17})$$

Eq. (A16) can be equivalently expressed by

$$\sum_{j=1}^3 (\bar{\Psi}\gamma_0\gamma_j\Psi)^2 = -(\bar{\Psi}\gamma_0\Psi)^2 + (\bar{\Psi}\Psi)^2 + (\bar{\Psi}\gamma_0\gamma_5\Psi)^2 - 2(\bar{\Psi}i\gamma_5\Psi)^2, \quad (\text{A18})$$

$$\sum_{\langle lk \rangle} (\bar{\Psi}i\gamma_l\gamma_k\Psi)^2 = -(\bar{\Psi}\gamma_0\Psi)^2 - 2(\bar{\Psi}\Psi)^2 + (\bar{\Psi}\gamma_0\gamma_5\Psi)^2 + (\bar{\Psi}i\gamma_5\Psi)^2, \quad (\text{A19})$$

$$\sum_{j=1}^3 (\bar{\Psi}i\gamma_5\gamma_j\Psi)^2 = -2(\bar{\Psi}\gamma_0\Psi)^2 - (\bar{\Psi}\Psi)^2 - (\bar{\Psi}\gamma_0\gamma_5\Psi)^2 - (\bar{\Psi}i\gamma_5\Psi)^2, \quad (\text{A20})$$

$$\sum_{j=1}^3 (\bar{\Psi}i\gamma_j\Psi)^2 = -(\bar{\Psi}\gamma_0\Psi)^2 + (\bar{\Psi}\Psi)^2 - 2(\bar{\Psi}\gamma_0\gamma_5\Psi)^2 + (\bar{\Psi}i\gamma_5\Psi)^2. \quad (\text{A21})$$

2. Fierz identity for 3D semi-DSM

For 3D semi-DSM, the interacting Lagrangian density is described by

$$\begin{aligned} \mathcal{L}_{\text{int}} = & g_1 (\bar{\Psi}\gamma_0\Psi)^2 + g_2 (\bar{\Psi}\Psi)^2 + g_{3\perp} \sum_{j=1}^2 (\bar{\Psi}\gamma_0\gamma_j\Psi)^2 + g_{3z} (\bar{\Psi}\gamma_0\gamma_3\Psi)^2 + g_4 (\bar{\Psi}\gamma_0\gamma_5\Psi)^2 + g_5 (\bar{\Psi}i\gamma_5\Psi)^2 \\ & + g_{6\perp} \sum_{\langle\langle lk \rangle\rangle} (\bar{\Psi}i\gamma_l\gamma_k\Psi)^2 + g_{6z} (\bar{\Psi}i\gamma_1\gamma_2\Psi)^2 + g_{7\perp} \sum_{j=1}^2 (\bar{\Psi}i\gamma_5\gamma_j\Psi)^2 + g_{7z} (\bar{\Psi}i\gamma_5\gamma_3\Psi)^2 \\ & + g_{8\perp} \sum_{j=1}^2 (\bar{\Psi}i\gamma_j\Psi)^2 + g_{8z} (\bar{\Psi}i\gamma_3\Psi)^2, \end{aligned} \quad (\text{A22})$$

where

$$\sum_{\langle\langle lk \rangle\rangle} (\bar{\Psi} i \gamma_l \gamma_k \Psi)^2 = \left[(\bar{\Psi} i \gamma_2 \gamma_3 \Psi)^2 + (\bar{\Psi} i \gamma_3 \gamma_1 \Psi)^2 \right]. \quad (\text{A23})$$

As shown in Eq. (A1), there are 8 four-fermion couplings for 3D DSM. However, we consider 12 kinds of four-fermion couplings as shown in Eq. (A22) for 3D semi-DSM, due to the anisotropy of the fermion dispersion.

Substituting each four-fermion coupling in Eq. (A22) into Eq. (A4), we could get 12 equations, which can be compactly expressed by

$$FX = 0, \quad (\text{A24})$$

where

$$X = \begin{pmatrix} (\bar{\Psi} \gamma_0 \Psi)^2 \\ (\bar{\Psi} \Psi)^2 \\ \sum_{j=1}^2 (\bar{\Psi} \gamma_0 \gamma_j \Psi)^2 \\ (\bar{\Psi} \gamma_0 \gamma_3 \Psi)^2 \\ (\bar{\Psi} \gamma_0 \gamma_5 \Psi)^2 \\ (\bar{\Psi} i \gamma_5 \Psi)^2 \\ \sum_{\langle\langle lk \rangle\rangle} (\bar{\Psi} i \gamma_l \gamma_k \Psi)^2 \\ (\bar{\Psi} i \gamma_1 \gamma_2 \Psi)^2 \\ \sum_{j=1}^2 (\bar{\Psi} i \gamma_5 \gamma_j \Psi)^2 \\ (\bar{\Psi} i \gamma_5 \gamma_3 \Psi)^2 \\ \sum_{j=1}^2 (\bar{\Psi} i \gamma_j \Psi)^2 \\ (\bar{\Psi} i \gamma_3 \Psi)^2 \end{pmatrix}, \quad (\text{A25})$$

and

$$F = \begin{pmatrix} 5 & 1 & 1 & 1 & 1 & 1 & 1 & 1 & 1 & 1 & 1 & 1 \\ 1 & 5 & -1 & -1 & -1 & -1 & 1 & 1 & 1 & 1 & -1 & -1 \\ 1 & -1 & 2 & -1 & -1 & 1 & 0 & 1 & 0 & -1 & 0 & 1 \\ 1 & -1 & -1 & 5 & -1 & 1 & 1 & -1 & -1 & 1 & 1 & -1 \\ 1 & -1 & -1 & -1 & 5 & -1 & -1 & -1 & 1 & 1 & 1 & 1 \\ 1 & -1 & 1 & 1 & -1 & 5 & -1 & -1 & 1 & 1 & -1 & -1 \\ 1 & 1 & 0 & 1 & -1 & -1 & 2 & -1 & 0 & -1 & 0 & 1 \\ 1 & 1 & 1 & -1 & -1 & -1 & -1 & 5 & -1 & 1 & 1 & -1 \\ 1 & 1 & 0 & -1 & 1 & 1 & 0 & -1 & 2 & -1 & 0 & -1 \\ 1 & 1 & -1 & 1 & 1 & 1 & -1 & 1 & -1 & 5 & -1 & 1 \\ 1 & -1 & 0 & 1 & 1 & -1 & 0 & 1 & 0 & -1 & 2 & -1 \\ 1 & -1 & 1 & -1 & 1 & -1 & 1 & -1 & -1 & 1 & -1 & 5 \end{pmatrix}. \quad (\text{A26})$$

It is easy to find that

$$\text{Rank}(F) = 7. \quad (\text{A27})$$

Then, the number of linearly independent couplings is

$$12 - \text{Rank}(F) = 5. \quad (\text{A28})$$

For convenience, we take the five couplings

$$(\bar{\Psi} \gamma_0 \Psi)^2, \quad (\bar{\Psi} \Psi)^2, \quad (\bar{\Psi} \gamma_0 \gamma_5 \Psi)^2, \quad (\bar{\Psi} i \gamma_5 \Psi)^2, \quad (\bar{\Psi} \gamma_0 \gamma_3 \Psi)^2, \quad (\text{A29})$$

as linearly independent couplings. The other couplings

$$\begin{aligned} & \sum_{j=1}^2 (\bar{\Psi}\gamma_0\gamma_j\Psi)^2, & \sum_{\langle\langle lk\rangle\rangle} (\bar{\Psi}i\gamma_l\gamma_k\Psi)^2, & (\bar{\Psi}i\gamma_1\gamma_2\Psi)^2, & \sum_{j=1}^2 (\bar{\Psi}i\gamma_5\gamma_j\Psi)^2, & (\bar{\Psi}i\gamma_5\gamma_3\Psi)^2, \\ & \sum_{j=1}^2 (\bar{\Psi}i\gamma_j\Psi)^2, & (\bar{\Psi}i\gamma_3\Psi)^2, & & & \end{aligned} \quad (\text{A30})$$

can be expressed by the five independent couplings shown in Eq. (A29). In order to obtain the concrete expressions for other couplings, we define

$$\tilde{X} = \begin{pmatrix} \sum_{j=1}^2 (\bar{\Psi}\gamma_0\gamma_j\Psi)^2 \\ \sum_{\langle\langle lk\rangle\rangle} (\bar{\Psi}i\gamma_l\gamma_k\Psi)^2 \\ (\bar{\Psi}i\gamma_1\gamma_2\Psi)^2 \\ \sum_{j=1}^2 (\bar{\Psi}i\gamma_5\gamma_j\Psi)^2 \\ (\bar{\Psi}i\gamma_5\gamma_3\Psi)^2 \\ \sum_{j=1}^2 (\bar{\Psi}i\gamma_j\Psi)^2 \\ (\bar{\Psi}i\gamma_3\Psi)^2 \\ (\bar{\Psi}\gamma_0\Psi)^2 \\ (\bar{\Psi}\Psi)^2 \\ (\bar{\Psi}\gamma_0\gamma_5\Psi)^2 \\ (\bar{\Psi}i\gamma_5\Psi)^2 \\ (\bar{\Psi}\gamma_0\gamma_3\Psi)^2 \end{pmatrix}. \quad (\text{A31})$$

It is easy to find that

$$\tilde{F}\tilde{X} = 0, \quad (\text{A32})$$

where

$$\tilde{F} = \begin{pmatrix} 1 & 1 & 1 & 1 & 1 & 1 & 1 & 5 & 1 & 1 & 1 & 1 \\ -1 & 1 & 1 & 1 & 1 & -1 & -1 & 1 & 5 & -1 & -1 & -1 \\ 2 & 0 & 1 & 0 & -1 & 0 & 1 & 1 & -1 & -1 & 1 & -1 \\ -1 & 1 & -1 & -1 & 1 & 1 & -1 & 1 & -1 & -1 & 1 & 5 \\ -1 & -1 & -1 & 1 & 1 & 1 & 1 & 1 & -1 & 5 & -1 & -1 \\ 1 & -1 & -1 & 1 & 1 & -1 & -1 & 1 & -1 & -1 & 5 & 1 \\ 0 & 2 & -1 & 0 & -1 & 0 & 1 & 1 & 1 & -1 & -1 & 1 \\ 1 & -1 & 5 & -1 & 1 & 1 & -1 & 1 & 1 & -1 & -1 & -1 \\ 0 & 0 & -1 & 2 & -1 & 0 & -1 & 1 & 1 & 1 & 1 & -1 \\ -1 & -1 & 1 & -1 & 5 & -1 & 1 & 1 & 1 & 1 & 1 & 1 \\ 0 & 0 & 1 & 0 & -1 & 2 & -1 & 1 & -1 & 1 & -1 & 1 \\ 1 & 1 & -1 & -1 & 1 & -1 & 5 & 1 & -1 & 1 & -1 & -1 \end{pmatrix}. \quad (\text{A33})$$

Carrying out a series of similarity transformations for \tilde{F} ,

$$\tilde{F} \rightarrow \tilde{F}', \quad (\text{A34})$$

we arrive

$$\tilde{F}'\tilde{X} = 0, \quad (\text{A35})$$

where

$$\tilde{F}' = \begin{pmatrix} 1 & 0 & 0 & 0 & 0 & 0 & 0 & 1 & -1 & -1 & 2 & 1 \\ 0 & 1 & 0 & 0 & 0 & 0 & 0 & 1 & 1 & -1 & 0 & 1 \\ 0 & 0 & 1 & 0 & 0 & 0 & 0 & 0 & 1 & 0 & -1 & -1 \\ 0 & 0 & 0 & 1 & 0 & 0 & 0 & 1 & 1 & 1 & 0 & -1 \\ 0 & 0 & 0 & 0 & 1 & 0 & 0 & 1 & 0 & 0 & 1 & 1 \\ 0 & 0 & 0 & 0 & 0 & 1 & 0 & 1 & -1 & 1 & 0 & 1 \\ 0 & 0 & 0 & 0 & 0 & 0 & 1 & 0 & 0 & 1 & -1 & -1 \\ 0 & 0 & 0 & 0 & 0 & 0 & 0 & 0 & 0 & 0 & 0 & 0 \\ 0 & 0 & 0 & 0 & 0 & 0 & 0 & 0 & 0 & 0 & 0 & 0 \\ 0 & 0 & 0 & 0 & 0 & 0 & 0 & 0 & 0 & 0 & 0 & 0 \\ 0 & 0 & 0 & 0 & 0 & 0 & 0 & 0 & 0 & 0 & 0 & 0 \\ 0 & 0 & 0 & 0 & 0 & 0 & 0 & 0 & 0 & 0 & 0 & 0 \\ 0 & 0 & 0 & 0 & 0 & 0 & 0 & 0 & 0 & 0 & 0 & 0 \end{pmatrix}. \quad (\text{A36})$$

Eq. (A35) can be also written as

$$\sum_{j=1}^2 (\bar{\Psi} \gamma_0 \gamma_j \Psi)^2 = -(\bar{\Psi} \gamma_0 \Psi)^2 + (\bar{\Psi} \Psi)^2 + (\bar{\Psi} \gamma_0 \gamma_5 \Psi)^2 - 2(\bar{\Psi} i \gamma_5 \Psi)^2 - (\bar{\Psi} \gamma_0 \gamma_3 \Psi)^2, \quad (\text{A37})$$

$$\sum_{\langle\langle lk \rangle\rangle} (\bar{\Psi} i \gamma_l \gamma_k \Psi)^2 = -(\bar{\Psi} \gamma_0 \Psi)^2 - (\bar{\Psi} \Psi)^2 + (\bar{\Psi} \gamma_0 \gamma_5 \Psi)^2 - (\bar{\Psi} \gamma_0 \gamma_3 \Psi)^2, \quad (\text{A38})$$

$$(\bar{\Psi} i \gamma_1 \gamma_2 \Psi)^2 = -(\bar{\Psi} \Psi)^2 + (\bar{\Psi} i \gamma_5 \Psi)^2 + (\bar{\Psi} \gamma_0 \gamma_3 \Psi)^2, \quad (\text{A39})$$

$$\sum_{j=1}^2 (\bar{\Psi} i \gamma_5 \gamma_j \Psi)^2 = -(\bar{\Psi} \gamma_0 \Psi)^2 - (\bar{\Psi} \Psi)^2 - (\bar{\Psi} \gamma_0 \gamma_5 \Psi)^2 + (\bar{\Psi} \gamma_0 \gamma_3 \Psi)^2, \quad (\text{A40})$$

$$(\bar{\Psi} i \gamma_5 \gamma_3 \Psi)^2 = -(\bar{\Psi} \gamma_0 \Psi)^2 - (\bar{\Psi} i \gamma_5 \Psi)^2 - (\bar{\Psi} \gamma_0 \gamma_3 \Psi)^2, \quad (\text{A41})$$

$$\sum_{j=1}^2 (\bar{\Psi} i \gamma_j \Psi)^2 = -(\bar{\Psi} \gamma_0 \Psi)^2 + (\bar{\Psi} \Psi)^2 - (\bar{\Psi} \gamma_0 \gamma_5 \Psi)^2 - (\bar{\Psi} \gamma_0 \gamma_3 \Psi)^2, \quad (\text{A42})$$

$$(\bar{\Psi} i \gamma_3 \Psi)^2 = -(\bar{\Psi} \gamma_0 \gamma_5 \Psi)^2 + (\bar{\Psi} i \gamma_5 \Psi)^2 + (\bar{\Psi} \gamma_0 \gamma_3 \Psi)^2. \quad (\text{A43})$$

Appendix B: Derivation of the RG equations for the strength of four-fermion couplings

1. Self-energy of the fermions

The fermion propagator reads as

$$G_0(i\omega, \mathbf{k}) = -\frac{i\omega\gamma_0 + iv(k_1\gamma_1 + k_2\gamma_2) + iAk_3^2\gamma_3}{\omega^2 + E_{\mathbf{k}}^2}, \quad (\text{B1})$$

where $E_{\mathbf{k}} = \sqrt{v^2 k_1^2 + A^2 k_3^4}$ with $k_1^2 = k_1^2 + k_2^2$. The self-energy of fermions resulting from Fig. 5(a) takes the form

$$\Sigma_1 = \sum_a g_a \int \frac{d\omega}{2\pi} \int' \frac{d^3\mathbf{k}}{(2\pi)^3} \Gamma_a G_0(\omega, \mathbf{k}) \Gamma_a, \quad (\text{B2})$$

where

$$\sum_a \equiv \sum_{a=1,2,4,5,3z}. \quad (\text{B3})$$

\int' represents that a momentum shell will be properly taken. Figure 5(b) induces the self-energy of fermions as following

$$\Sigma_2 = \sum_a g_a \int \frac{d\omega}{2\pi} \int' \frac{d^3\mathbf{k}}{(2\pi)^3} \text{Tr} [G_0(\omega, \mathbf{k}) \Gamma_a]. \quad (\text{B4})$$

Substituting Eq. (B1) into Eqs. (B2) and (B4), we obtain

$$\Sigma_1 = 0, \quad (\text{B5})$$

$$\Sigma_2 = 0. \quad (\text{B6})$$

It should be notice that a generated constant term in Σ_1 has been discarded. The generated constant term in self-energy is also discarded in the study about long-range Coulomb interaction in 3D semi-DSM [38]. According to Eqs. (B5) and (B6), the fermion propagator is not renormalized by the four-fermion interactions to one-loop order.

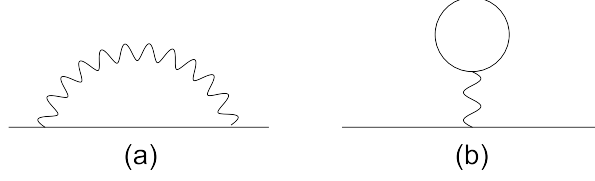


FIG. 5: Feynman diagrams for the self-energies of fermions induced by four-fermion interactions. Solid line represents the fermion propagator, and wavy line stands for the four-fermion interaction.

2. One-loop corrections for the four-fermion couplings

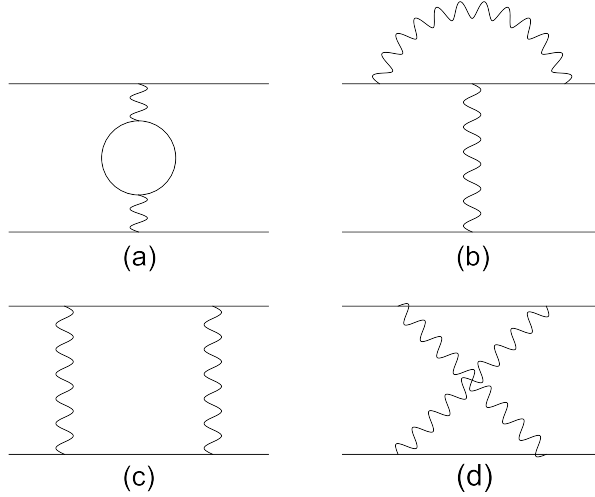


FIG. 6: One-loop Feynman diagrams for the corrections to the four-fermion couplings.

Fig. 6(a) leads to the correction

$$V_a^{(1)} = -2g_a^2 (\bar{\Psi}\Gamma_a\Psi)^2 \int_{-\infty}^{+\infty} \frac{d\omega}{2\pi} \int' \frac{d^3\mathbf{k}}{(2\pi)^3} \text{Tr} [\Gamma_a G_0(i\omega, \mathbf{k}) \Gamma_a G_0(i\omega, \mathbf{k})]. \quad (\text{B7})$$

Fig. 6(b) results in the correction

$$V_a^{(2)} = \sum_b V_{ab}^{(2)}, \quad (\text{B8})$$

where

$$V_a^{(2)} = 4g_a g_b (\bar{\Psi}\Gamma_a\Psi) \int_{-\infty}^{+\infty} \frac{d\omega}{2\pi} \int' \frac{d^3\mathbf{k}}{(2\pi)^3} (\bar{\Psi}\Gamma_b G_0(i\omega, \mathbf{k}) \Gamma_a G_0(i\omega, \mathbf{k}) \Gamma_b \Psi). \quad (\text{B9})$$

The Figs. 6(c) and 6(d) induce the correction

$$V^{(3)+(4)} = \sum_a \sum_{a \leq b} V_{ab}^{(3)+(4)}, \quad (\text{B10})$$

where

$$V_{ab}^{(3)+(4)} = 4g_a g_b \int_{-\infty}^{+\infty} \frac{d\omega}{2\pi} \int' \frac{d^3\mathbf{k}}{(2\pi)^3} (\bar{\Psi} \Gamma_a G_0(i\omega, \mathbf{k}) \Gamma_b \Psi) \bar{\Psi} [\Gamma_b G_0(i\omega, \mathbf{k}) \Gamma_a + \Gamma_a G_0(-i\omega, -\mathbf{k}) \Gamma_b] \Psi. \quad (\text{B11})$$

Substituting Eq. (B1) into Eq. (B7), we obtain

$$V_a^{(1)} = \delta g_a^{(1)} (\bar{\Psi} \Gamma_a \Psi)^2, \quad (\text{B12})$$

where

$$\delta g_1^{(1)} = 0, \quad (\text{B13})$$

$$\delta g_2^{(1)} = g_2^2 \frac{2\Lambda^{\frac{3}{2}}}{\pi^2 v^2 \sqrt{A}} \ell, \quad (\text{B14})$$

$$\delta g_4^{(1)} = 0, \quad (\text{B15})$$

$$\delta g_5^{(1)} = g_5^2 \frac{2\Lambda^{\frac{3}{2}}}{\pi^2 v^2 \sqrt{A}} \ell, \quad (\text{B16})$$

$$\delta g_{3z}^{(1)} = g_{3z}^2 \frac{2\Lambda^{\frac{3}{2}}}{5\pi^2 v^2 \sqrt{A}} \ell. \quad (\text{B17})$$

Substituting Eq. (B1) into Eqs. (B8) and (B9), we find that the contribution from Fig. 6(b) can be written as

$$V_a^{(2)} = \delta g_a^{(2)} (\bar{\Psi} \Gamma_a \Psi)^2, \quad (\text{B18})$$

where

$$\delta g_1^{(2)} = 0, \quad (\text{B19})$$

$$\delta g_2^{(2)} = (-g_2 g_1 - g_2^2 + g_2 g_4 + g_2 g_5 + g_2 g_{3z}) \frac{\Lambda^{\frac{3}{2}}}{\pi^2 v^2 \sqrt{A}} \ell, \quad (\text{B20})$$

$$\delta g_4^{(2)} = 0, \quad (\text{B21})$$

$$\delta g_5^{(2)} = (-g_5 g_1 + g_5 g_2 + g_5 g_4 - g_5^2 - g_5 g_{3z}) \frac{\Lambda^{\frac{3}{2}}}{\pi^2 v^2 \sqrt{A}} \ell, \quad (\text{B22})$$

$$\delta g_{3z}^{(2)} = (-g_{3z} g_1 + g_{3z} g_2 + g_{3z} g_4 - g_{3z} g_5 - g_{3z}^2) \frac{\Lambda^{\frac{3}{2}}}{5\pi^2 v^2 \sqrt{A}} \ell. \quad (\text{B23})$$

Substituting Eq. (B1) into Eq. (B11), the contribution from Figs. 6(c) and 6(d) can be written as

$$V_{1,1}^{(3)+(4)} = g_1^2 \frac{\Lambda^{\frac{3}{2}}}{5\pi^2 v^2 \sqrt{A}} \ell (\bar{\Psi} i\gamma_3 \Psi)^2, \quad (\text{B24})$$

$$V_{2,2}^{(3)+(4)} = g_2^2 \frac{\Lambda^{\frac{3}{2}}}{5\pi^2 v^2 \sqrt{A}} \ell (\bar{\Psi} i\gamma_3 \Psi)^2, \quad (\text{B25})$$

$$V_{4,4}^{(3)+(4)} = g_4^2 \frac{\Lambda^{\frac{3}{2}}}{5\pi^2 v^2 \sqrt{A}} \ell (\bar{\Psi} i\gamma_3 \Psi)^2, \quad (\text{B26})$$

$$V_{5,5}^{(3)+(4)} = g_5^2 \frac{\Lambda^{\frac{3}{2}}}{5\pi^2 v^2 \sqrt{A}} \ell (\bar{\Psi} i\gamma_3 \Psi)^2, \quad (\text{B27})$$

$$V_{3z,3z}^{(3)+(4)} = g_{3z}^2 \frac{\Lambda^{\frac{3}{2}}}{5\pi^2 v^2 \sqrt{A}} \ell (\bar{\Psi} i\gamma_3 \Psi)^2, \quad (\text{B28})$$

$$V_{1,2}^{(3)+(4)} = g_1 g_2 \frac{2\Lambda^{\frac{3}{2}}}{5\pi^2 v^2 \sqrt{A}} \ell \sum_{j=1}^2 (\bar{\Psi} \gamma_0 \gamma_j \Psi)^2, \quad (\text{B29})$$

$$V_{1,4}^{(3)+(4)} = g_1 g_4 \frac{\Lambda^{\frac{3}{2}}}{5\pi^2 v^2 \sqrt{A}} \ell (\bar{\Psi} i \gamma_5 \gamma_3 \Psi)^2, \quad (\text{B30})$$

$$V_{1,5}^{(3)+(4)} = g_1 g_5 \frac{2\Lambda^{\frac{3}{2}}}{5\pi^2 v^2 \sqrt{A}} \ell \sum_{\langle\langle lk \rangle\rangle} (\bar{\Psi} i \gamma_l \gamma_k \Psi)^2, \quad (\text{B31})$$

$$V_{1,3z}^{(3)+(4)} = 0, \quad (\text{B32})$$

$$V_{2,4}^{(3)+(4)} = -g_2 g_4 \frac{\Lambda^{\frac{3}{2}}}{\pi^2 v^2 \sqrt{A}} \ell (\bar{\Psi} i \gamma_5 \Psi)^2 + g_2 g_4 \frac{\Lambda^{\frac{3}{2}}}{5\pi^2 v^2 \sqrt{A}} \ell (\bar{\Psi} i \gamma_1 \gamma_2 \Psi)^2, \quad (\text{B33})$$

$$V_{2,5}^{(3)+(4)} = -g_2 g_5 \frac{\Lambda^{\frac{3}{2}}}{\pi^2 v^2 \sqrt{A}} \ell (\bar{\Psi} \gamma_0 \gamma_5 \Psi)^2 + g_2 g_5 \sum_{j=1}^2 \frac{2\Lambda^{\frac{3}{2}}}{5\pi^2 v^2 \sqrt{A}} \ell (\bar{\Psi} i \gamma_5 \gamma_j \Psi)^2, \quad (\text{B34})$$

$$V_{2,3z}^{(3)+(4)} = -g_2 g_{3z} \frac{\Lambda^{\frac{3}{2}}}{\pi^2 v^2 \sqrt{A}} \ell (\bar{\Psi} i \gamma_3 \Psi)^2, \quad (\text{B35})$$

$$V_{4,5}^{(3)+(4)} = -g_4 g_5 \frac{\Lambda^{\frac{3}{2}}}{\pi^2 v^2 \sqrt{A}} \ell (\bar{\Psi} \Psi)^2 + g_4 g_5 \frac{\Lambda^{\frac{3}{2}}}{5\pi^2 v^2 \sqrt{A}} \ell (\bar{\Psi} \gamma_0 \gamma_3 \Psi)^2, \quad (\text{B36})$$

$$V_{4,3z}^{(3)+(4)} = -g_4 g_{3z} \frac{\Lambda^{\frac{3}{2}}}{\pi^2 v^2 \sqrt{A}} \ell (\bar{\Psi} i \gamma_1 \gamma_2 \Psi)^2 + g_4 g_{3z} \sum_{j=1}^2 \frac{2\Lambda^{\frac{3}{2}}}{5\pi^2 v^2 \sqrt{A}} \ell (\bar{\Psi} \gamma_0 \gamma_j \Psi)^2 + g_4 g_{3z} \frac{\Lambda^{\frac{3}{2}}}{5\pi^2 v^2 \sqrt{A}} \ell (\bar{\Psi} i \gamma_5 \Psi)^2, \quad (\text{B37})$$

$$V_{5,3z}^{(3)+(4)} = g_5 g_{3z} \sum_{j=1}^2 \frac{2\Lambda^{\frac{3}{2}}}{5\pi^2 v^2 \sqrt{A}} \ell (\bar{\Psi} i \gamma_j \Psi)^2 + g_5 g_{3z} \frac{\Lambda^{\frac{3}{2}}}{5\pi^2 v^2 \sqrt{A}} \ell (\bar{\Psi} \gamma_0 \gamma_5 \Psi)^2. \quad (\text{B38})$$

Using the relations shown in Eqs. (A37)-(A43), we further get

$$V_{1,1}^{(3)+(4)} = g_0^2 \frac{\Lambda^{\frac{3}{2}}}{5\pi^2 v^2 \sqrt{A}} \ell \left[-(\bar{\Psi} \gamma_0 \gamma_5 \Psi)^2 + (\bar{\Psi} i \gamma_5 \Psi)^2 + (\bar{\Psi} \gamma_0 \gamma_3 \Psi)^2 \right], \quad (\text{B39})$$

$$V_{2,2}^{(3)+(4)} = g_2^2 \frac{\Lambda^{\frac{3}{2}}}{5\pi^2 v^2 \sqrt{A}} \ell \left[-(\bar{\Psi} \gamma_0 \gamma_5 \Psi)^2 + (\bar{\Psi} i \gamma_5 \Psi)^2 + (\bar{\Psi} \gamma_0 \gamma_3 \Psi)^2 \right], \quad (\text{B40})$$

$$V_{4,4}^{(3)+(4)} = g_4^2 \frac{\Lambda^{\frac{3}{2}}}{5\pi^2 v^2 \sqrt{A}} \ell \left[-(\bar{\Psi} \gamma_0 \gamma_5 \Psi)^2 + (\bar{\Psi} i \gamma_5 \Psi)^2 + (\bar{\Psi} \gamma_0 \gamma_3 \Psi)^2 \right], \quad (\text{B41})$$

$$V_{5,5}^{(3)+(4)} = g_5^2 \frac{\Lambda^{\frac{3}{2}}}{5\pi^2 v^2 \sqrt{A}} \ell \left[-(\bar{\Psi} \gamma_0 \gamma_5 \Psi)^2 + (\bar{\Psi} i \gamma_5 \Psi)^2 + (\bar{\Psi} \gamma_0 \gamma_3 \Psi)^2 \right], \quad (\text{B42})$$

$$V_{3z,3z}^{(3)+(4)} = g_{3z}^2 \frac{\Lambda^{\frac{3}{2}}}{5\pi^2 v^2 \sqrt{A}} \ell \left[-(\bar{\Psi} \gamma_0 \gamma_5 \Psi)^2 + (\bar{\Psi} i \gamma_5 \Psi)^2 + (\bar{\Psi} \gamma_0 \gamma_3 \Psi)^2 \right], \quad (\text{B43})$$

$$V_{1,2}^{(3)+(4)} = g_1 g_2 \frac{2\Lambda^{\frac{3}{2}}}{5\pi^2 v^2 \sqrt{A}} \ell \left[-(\bar{\Psi} \gamma_0 \Psi)^2 + (\bar{\Psi} \Psi)^2 + (\bar{\Psi} \gamma_0 \gamma_5 \Psi)^2 - 2(\bar{\Psi} i \gamma_5 \Psi)^2 - (\bar{\Psi} \gamma_0 \gamma_3 \Psi)^2 \right], \quad (\text{B44})$$

$$V_{1,4}^{(3)+(4)} = g_1 g_4 \frac{\Lambda^{\frac{3}{2}}}{5\pi^2 v^2 \sqrt{A}} \ell \left[-(\bar{\Psi} \gamma_0 \Psi)^2 - (\bar{\Psi} i \gamma_5 \Psi)^2 - (\bar{\Psi} \gamma_0 \gamma_3 \Psi)^2 \right], \quad (\text{B45})$$

$$V_{1,5}^{(3)+(4)} = g_1 g_5 \frac{2\Lambda^{\frac{3}{2}}}{5\pi^2 v^2 \sqrt{A}} \ell \left[-(\bar{\Psi} \gamma_0 \Psi)^2 - (\bar{\Psi} \Psi)^2 + (\bar{\Psi} \gamma_0 \gamma_5 \Psi)^2 - (\bar{\Psi} \gamma_0 \gamma_3 \Psi)^2 \right], \quad (\text{B46})$$

$$V_{1,3z}^{(3)+(4)} = 0, \quad (\text{B47})$$

$$V_{2,4}^{(3)+(4)} = g_2 g_4 \frac{\Lambda^{\frac{3}{2}}}{5\pi^2 v^2 \sqrt{A}} \ell \left[-(\bar{\Psi} \Psi)^2 - 4(\bar{\Psi} i \gamma_5 \Psi)^2 + (\bar{\Psi} \gamma_0 \gamma_3 \Psi)^2 \right], \quad (\text{B48})$$

$$V_{2,5}^{(3)+(4)} = g_2 g_5 \frac{2\Lambda^{\frac{3}{2}}}{5\pi^2 v^2 \sqrt{A}} \ell \left[-(\bar{\Psi} \gamma_0 \Psi)^2 - (\bar{\Psi} \Psi)^2 - \frac{7}{2}(\bar{\Psi} \gamma_0 \gamma_5 \Psi)^2 + (\bar{\Psi} \gamma_0 \gamma_3 \Psi)^2 \right], \quad (\text{B49})$$

$$V_{2,3z}^{(3)+(4)} = -g_2 g_{3z} \frac{\Lambda^{\frac{3}{2}}}{\pi^2 v^2 \sqrt{A}} \ell \left[-(\bar{\Psi} \gamma_0 \gamma_5 \Psi)^2 + (\bar{\Psi} i \gamma_5 \Psi)^2 + (\bar{\Psi} \gamma_0 \gamma_3 \Psi)^2 \right], \quad (\text{B50})$$

$$V_{4,5}^{(3)+(4)} = g_4 g_5 \frac{\Lambda^{\frac{3}{2}}}{5\pi^2 v^2 \sqrt{A}} \ell \left[-5 (\bar{\Psi}\Psi)^2 + (\bar{\Psi}\gamma_0\gamma_3\Psi)^2 \right] \quad (\text{B51})$$

$$V_{4,3z}^{(3)+(4)} = g_4 g_{3z} \frac{2\Lambda^{\frac{3}{2}}}{5\pi^2 v^2 \sqrt{A}} \ell \left[-(\bar{\Psi}\gamma_0\Psi)^2 + \frac{7}{2} (\bar{\Psi}\Psi)^2 + (\bar{\Psi}\gamma_0\gamma_5\Psi)^2 - 4 (\bar{\Psi}i\gamma_5\Psi)^2 - \frac{7}{2} (\bar{\Psi}\gamma_0\gamma_3\Psi)^2 \right], \quad (\text{B52})$$

$$V_{5,3z}^{(3)+(4)} = g_5 g_{3z} \frac{2\Lambda^{\frac{3}{2}}}{5\pi^2 v^2 \sqrt{A}} \ell \left[-(\bar{\Psi}\gamma_0\Psi)^2 + (\bar{\Psi}\Psi)^2 - \frac{1}{2} (\bar{\Psi}\gamma_0\gamma_5\Psi)^2 - (\bar{\Psi}\gamma_0\gamma_3\Psi)^2 \right]. \quad (\text{B53})$$

Thus, the contribution from Figs. 6(c) and 6(d) is given by

$$\begin{aligned} V^{(3)+(4)} &= \sum_{a=1,2,4,5,3z} \sum_{a \leq b} V_{ab}^{(3)+(4)} \\ &= \sum_{a=1,2,4,5,3z} \delta g_a^{(3)+(4)} (\bar{\Psi}\Gamma_a\Psi)^2, \end{aligned} \quad (\text{B54})$$

where

$$\delta g_1^{(3)+(4)} = \left(-g_1 g_2 - \frac{1}{2} g_1 g_4 - g_1 g_5 - g_2 g_5 - g_4 g_{3z} - g_5 g_{3z} \right) \frac{2\Lambda^{\frac{3}{2}}}{5\pi^2 v^2 \sqrt{A}} \ell, \quad (\text{B55})$$

$$\delta g_2^{(3)+(4)} = \left(g_1 g_2 - g_1 g_5 - \frac{1}{2} g_2 g_4 - g_2 g_5 - \frac{5}{2} g_4 g_5 + \frac{7}{2} g_4 g_{3z} + g_5 g_{3z} \right) \frac{2\Lambda^{\frac{3}{2}}}{5\pi^2 v^2 \sqrt{A}} \ell, \quad (\text{B56})$$

$$\begin{aligned} \delta g_4^{(3)+(4)} &= \left(-\frac{1}{2} g_1^2 - \frac{1}{2} g_2^2 - \frac{1}{2} g_4^2 - \frac{1}{2} g_5^2 - \frac{1}{2} g_{3z}^2 + g_1 g_2 + g_1 g_5 - \frac{7}{2} g_2 g_5 + \frac{5}{2} g_2 g_{3z} + g_4 g_{3z} - \frac{1}{2} g_5 g_{3z} \right) \\ &\quad \times \frac{2\Lambda^{\frac{3}{2}}}{5\pi^2 v^2 \sqrt{A}} \ell, \end{aligned} \quad (\text{B57})$$

$$\delta g_5^{(3)+(4)} = \left(\frac{1}{2} g_1^2 + \frac{1}{2} g_2^2 + \frac{1}{2} g_4^2 + \frac{1}{2} g_5^2 + \frac{1}{2} g_{3z}^2 - 2g_1 g_2 - \frac{1}{2} g_1 g_4 - 2g_2 g_4 - \frac{5}{2} g_2 g_{3z} - 4g_4 g_{3z} \right) \frac{2\Lambda^{\frac{3}{2}}}{5\pi^2 v^2 \sqrt{A}} \ell, \quad (\text{B58})$$

$$\begin{aligned} \delta g_{3z}^{(3)+(4)} &= \left(\frac{1}{2} g_1^2 + \frac{1}{2} g_2^2 + \frac{1}{2} g_4^2 + \frac{1}{2} g_5^2 + \frac{1}{2} g_{3z}^2 - g_1 g_2 - \frac{1}{2} g_1 g_4 - g_1 g_5 + \frac{1}{2} g_2 g_4 + g_2 g_5 - \frac{5}{2} g_2 g_{3z} + \frac{1}{2} g_4 g_5 \right. \\ &\quad \left. - \frac{7}{2} g_4 g_{3z} - g_5 g_{3z} \right) \frac{2\Lambda^{\frac{3}{2}}}{5\pi^2 v^2 \sqrt{A}} \ell. \end{aligned} \quad (\text{B59})$$

From the above results, we obtain

$$\delta g_a = \delta g_a^{(1)} + \delta g_a^{(2)} + \delta g_a^{(3)+(4)}. \quad (\text{B60})$$

Concretely,

$$\delta g_1 = \left(-g_1 g_2 - \frac{1}{2} g_1 g_4 - g_1 g_5 - g_2 g_5 - g_4 g_{3z} - g_5 g_{3z} \right) \frac{2\Lambda^{\frac{3}{2}}}{5\pi^2 v^2 \sqrt{A}} \ell, \quad (\text{B61})$$

$$\delta g_2 = \left(\frac{5}{2} g_2^2 - \frac{3}{2} g_1 g_2 - g_1 g_5 + 2g_2 g_4 + \frac{3}{2} g_2 g_5 + \frac{5}{2} g_2 g_{3z} - \frac{5}{2} g_4 g_5 + \frac{7}{2} g_4 g_{3z} + g_5 g_{3z} \right) \frac{2\Lambda^{\frac{3}{2}}}{5\pi^2 v^2 \sqrt{A}} \ell, \quad (\text{B62})$$

$$\delta g_4 = \left(-\frac{1}{2} g_1^2 - \frac{1}{2} g_2^2 - \frac{1}{2} g_4^2 - \frac{1}{2} g_5^2 - \frac{1}{2} g_{3z}^2 + g_1 g_2 + g_1 g_5 - \frac{7}{2} g_2 g_5 + \frac{5}{2} g_2 g_{3z} + g_4 g_{3z} - \frac{1}{2} g_5 g_{3z} \right) \frac{2\Lambda^{\frac{3}{2}}}{5\pi^2 v^2 \sqrt{A}} \ell, \quad (\text{B63})$$

$$\begin{aligned} \delta g_5 &= \left(\frac{1}{2} g_1^2 + \frac{1}{2} g_2^2 + \frac{1}{2} g_4^2 + 3g_5^2 + \frac{1}{2} g_{3z}^2 - 2g_1 g_2 - \frac{1}{2} g_1 g_4 - \frac{5}{2} g_1 g_5 - 2g_2 g_4 + \frac{5}{2} g_2 g_5 - \frac{5}{2} g_2 g_{3z} + \frac{5}{2} g_4 g_5 - 4g_4 g_{3z} \right. \\ &\quad \left. - \frac{5}{2} g_5 g_{3z} \right) \frac{2\Lambda^{\frac{3}{2}}}{5\pi^2 v^2 \sqrt{A}} \ell, \end{aligned} \quad (\text{B64})$$

$$\begin{aligned} \delta g_{3z} &= \left(\frac{1}{2} g_1^2 + \frac{1}{2} g_2^2 + \frac{1}{2} g_4^2 + \frac{1}{2} g_5^2 + g_{3z}^2 - g_1 g_2 - \frac{1}{2} g_1 g_4 - g_1 g_5 - \frac{1}{2} g_1 g_{3z} + \frac{1}{2} g_2 g_4 + g_2 g_5 - 2g_2 g_{3z} + \frac{1}{2} g_4 g_5 \right. \\ &\quad \left. - 3g_4 g_{3z} - \frac{3}{2} g_5 g_{3z} \right) \frac{2\Lambda^{\frac{3}{2}}}{5\pi^2 v^2 \sqrt{A}} \ell. \end{aligned} \quad (\text{B65})$$

3. Scaling transformations

The free action of fermions is

$$S_\Psi = \int \frac{d\omega}{2\pi} \frac{d^3\mathbf{k}}{(2\pi)^3} \bar{\Psi}(\omega, \mathbf{k}) (i\omega\gamma_0 + ivk_1\gamma_1 + ivk_2\gamma_2 + iAk_3^2\gamma_3) \Psi(\omega, \mathbf{k}). \quad (\text{B66})$$

The fermion self-energy induced by four-fermion interactions to one-loop order vanishes. Thus, the form of action S_Ψ is not changed. Employing the transformations

$$\omega = \omega' e^{-\ell}, \quad (\text{B67})$$

$$k_1 = k'_1 e^{-\ell}, \quad (\text{B68})$$

$$k_2 = k'_2 e^{-\ell}, \quad (\text{B69})$$

$$k_3 = k'_3 e^{-\frac{\ell}{2}}, \quad (\text{B70})$$

$$v = v', \quad (\text{B71})$$

$$A = A', \quad (\text{B72})$$

$$\Psi = \Psi' e^{\frac{3}{4}\ell}, \quad (\text{B73})$$

the action becomes

$$S_{\Psi'} = \int \frac{d\omega'}{2\pi} \frac{d^3\mathbf{k}'}{(2\pi)^3} \bar{\Psi}'(\omega', \mathbf{k}') (i\omega'\gamma_0 + iv'k'_1\gamma_1 + iv'k'_2\gamma_2 + iA'k'_3{}^2\gamma_3) \Psi'(\omega', \mathbf{k}'), \quad (\text{B74})$$

which has the same form as the original action.

The original action of four-fermion interactions takes the form

$$S_{\Psi^4} = \sum_{a=1,2,4,5,3z} g_a \int \frac{d\omega_1}{2\pi} \frac{d^3\mathbf{k}_1}{(2\pi)^3} \frac{d\omega_2}{2\pi} \frac{d^3\mathbf{k}_2}{(2\pi)^3} \frac{d\omega_3}{2\pi} \frac{d^3\mathbf{k}_3}{(2\pi)^3} \bar{\Psi}(\omega_1, \mathbf{k}_1) \Gamma_a \Psi(\omega_2, \mathbf{k}_2) \bar{\Psi}(\omega_3, \mathbf{k}_3) \Gamma_a \\ \times \Psi(\omega_1 - \omega_2 + \omega_3, \mathbf{k}_1 - \mathbf{k}_2 + \mathbf{k}_3). \quad (\text{B75})$$

Including the one-loop order correction, the action becomes

$$S_{\Psi^4} = \sum_{a=1,2,4,5,3z} (g_a + \delta g_a) \int \frac{d\omega_1}{2\pi} \frac{d^3\mathbf{k}_1}{(2\pi)^3} \frac{d\omega_2}{2\pi} \frac{d^3\mathbf{k}_2}{(2\pi)^3} \frac{d\omega_3}{2\pi} \frac{d^3\mathbf{k}_3}{(2\pi)^3} \bar{\Psi}(\omega_1, \mathbf{k}_1) \Gamma_a \Psi(\omega_2, \mathbf{k}_2) \bar{\Psi}(\omega_3, \mathbf{k}_3) \Gamma_a \\ \times \Psi(\omega_1 - \omega_2 + \omega_3, \mathbf{k}_1 - \mathbf{k}_2 + \mathbf{k}_3). \quad (\text{B76})$$

Utilizing the transformations Eqs. (B67)-(B70) and (B73), we get

$$S_{\Psi'^4} = \sum_{a=1,2,4,5,3z} (g_a + \delta g_a) e^{-\frac{3}{2}\ell} \int \frac{d\omega'_1}{2\pi} \frac{d^3\mathbf{k}'_1}{(2\pi)^3} \frac{d\omega'_2}{2\pi} \frac{d^3\mathbf{k}'_2}{(2\pi)^3} \frac{d\omega'_3}{2\pi} \frac{d^3\mathbf{k}'_3}{(2\pi)^3} \bar{\Psi}'(\omega'_1, \mathbf{k}'_1) \Gamma_a \Psi'(\omega'_2, \mathbf{k}'_2) \bar{\Psi}'(\omega'_3, \mathbf{k}'_3) \Gamma_a \\ \times \Psi'(\omega'_1 - \omega'_2 + \omega'_3, \mathbf{k}'_1 - \mathbf{k}'_2 + \mathbf{k}'_3). \quad (\text{B77})$$

Let

$$g'_a = (g_a + \delta g_a) e^{-\frac{3}{2}\ell} \approx g_a - \frac{3}{2}g_a\ell + \delta g_a, \quad (\text{B78})$$

we obtain

$$S_{\Psi'^4} = \sum_{a=1,2,4,5,3z} g'_a \int \frac{d\omega'_1}{2\pi} \frac{d^3\mathbf{k}'_1}{(2\pi)^3} \frac{d\omega'_2}{2\pi} \frac{d^3\mathbf{k}'_2}{(2\pi)^3} \frac{d\omega'_3}{2\pi} \frac{d^3\mathbf{k}'_3}{(2\pi)^3} \bar{\Psi}'(\omega'_1, \mathbf{k}'_1) \Gamma_a \Psi'(\omega'_2, \mathbf{k}'_2) \bar{\Psi}'(\omega'_3, \mathbf{k}'_3) \Gamma_a \\ \times \Psi'(\omega'_1 - \omega'_2 + \omega'_3, \mathbf{k}'_1 - \mathbf{k}'_2 + \mathbf{k}'_3)$$

which recovers the original form of the action.

From Eq. (B78), we get the RG equation for g_a as following

$$\frac{dg_a}{d\ell} = -\frac{3}{2}g_a + \frac{d\delta g_a}{d\ell}. \quad (\text{B79})$$

Substituting Eqs. (B61)-(B65) into Eq. (B79), we find

$$\frac{dg_1}{d\ell} = -\frac{3}{2}g_1 - \frac{2}{5}g_1 \left(g_2 + \frac{1}{2}g_4 + g_5 \right) - \frac{2}{5}(g_2g_5 + g_4g_{3z} + g_5g_{3z}), \quad (\text{B80})$$

$$\frac{dg_2}{d\ell} = -\frac{3}{2}g_2 + g_2^2 + g_2 \left(-\frac{3}{5}g_1 + \frac{4}{5}g_4 + \frac{3}{5}g_5 + g_{3z} \right) - \frac{2}{5}g_1g_5 + g_4 \left(-g_5 + \frac{7}{5}g_{3z} \right) + \frac{2}{5}g_5g_{3z}, \quad (\text{B81})$$

$$\frac{dg_4}{d\ell} = -\frac{3}{2}g_4 - \frac{1}{5}g_4^2 - \frac{1}{5}(g_1^2 + g_2^2 + g_5^2 + g_{3z}^2) + \frac{2}{5}g_4g_{3z} + \frac{2}{5}g_1(g_2 + g_5) + g_2 \left(-\frac{7}{5}g_5 + g_{3z} \right) - \frac{1}{5}g_5g_{3z}, \quad (\text{B82})$$

$$\begin{aligned} \frac{dg_5}{d\ell} = & -\frac{3}{2}g_5 + \frac{6}{5}g_5^2 + \frac{1}{5}(g_1^2 + g_2^2 + g_4^2 + g_{3z}^2) + g_5(-g_1 + g_2 + g_4 - g_{3z}) - \frac{2}{5}g_1 \left(2g_2 + \frac{1}{2}g_4 \right) - g_2 \left(\frac{4}{5}g_4 + g_{3z} \right) \\ & - \frac{8}{5}g_4g_{3z}, \end{aligned} \quad (\text{B83})$$

$$\begin{aligned} \frac{dg_{3z}}{d\ell} = & -\frac{3}{2}g_{3z} + \frac{2}{5}g_{3z}^2 + \frac{1}{5}(g_1^2 + g_2^2 + g_4^2 + g_5^2) - \frac{2}{5}g_{3z} \left(\frac{1}{2}g_1 + 2g_2 + 3g_4 + \frac{3}{2}g_5 \right) - \frac{2}{5}g_1 \left(g_2 + \frac{1}{2}g_4 + g_5 \right) \\ & + \frac{2}{5}g_2 \left(\frac{1}{2}g_4 + g_5 \right) + \frac{1}{5}g_4g_5. \end{aligned} \quad (\text{B84})$$

The redefinition

$$\frac{\Lambda^{\frac{3}{2}}g_a}{\pi^2v^2\sqrt{A}} \rightarrow g_a, \quad (\text{B85})$$

has been employed.

Appendix C: Susceptibility of source terms

We consider the Lagrangian for the source terms as following

$$\begin{aligned} \mathcal{L}_s = & \Delta_1 \bar{\Psi} \gamma_0 \Psi + \Delta_2 \bar{\Psi} \Psi + \Delta_{3\perp} \sum_{j=1}^2 \bar{\Psi} \gamma_0 \gamma_j \Psi + \Delta_{3z} \bar{\Psi} \gamma_0 \gamma_3 \Psi + \Delta_4 \bar{\Psi} \gamma_0 \gamma_5 \Psi + \Delta_5 \bar{\Psi} i \gamma_5 \Psi + \Delta_{6\perp} \sum_{\langle lk \rangle} (\bar{\Psi} i \gamma_l \gamma_k \Psi) \\ & + \Delta_{6z} \bar{\Psi} i \gamma_1 \gamma_2 \Psi + \Delta_{7\perp} \sum_{j=1}^2 \bar{\Psi} i \gamma_5 \gamma_j \Psi + \Delta_{7z} \bar{\Psi} i \gamma_5 \gamma_3 \Psi + \Delta_{8\perp} \sum_{j=1}^2 \bar{\Psi} i \gamma_j \Psi + \Delta_{8z} \bar{\Psi} i \gamma_3 \Psi + \Delta_S \Psi^\dagger i \gamma_0 \gamma_5 \gamma_2 \Psi^* \\ & + \Delta_{op} \Psi^\dagger i \gamma_0 \gamma_2 \Psi^* + \Delta_{V,1} \Psi^\dagger \gamma_3 \Psi^* + \Delta_{V,2} \Psi^\dagger i \gamma_0 \gamma_5 \Psi^* + \Delta_{V,3} \Psi^\dagger \gamma_1 \Psi^* + \Delta_{V,0} \Psi^\dagger i \gamma_0 \gamma_2 \gamma_3 \Psi^*. \end{aligned} \quad (\text{C1})$$

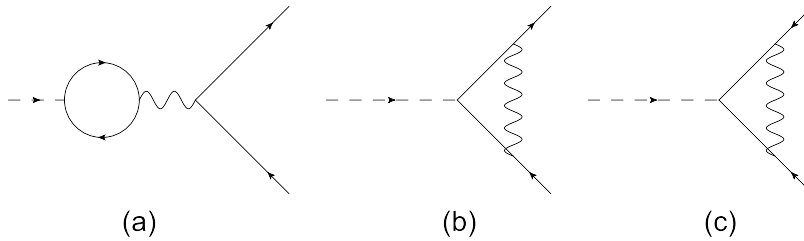


FIG. 7: (a) and (b): One-loop Feynman diagrams for the corrections to the source terms in particle-hole channel. (c): One-loop Feynman diagram for the correction to the source terms in particle-particle channel.

1. One-loop order corrections for source terms in particle-hole channel

There are two one-loop Feynman diagrams lead to the correction for source terms in particle-hole channel. The one-loop correction for the source term Δ_X from Fig. 7(a) is given by

$$W_{\Delta_X}^{(1)} = -2\Delta_X g_X (\bar{\Psi} \Gamma_X \Psi) \sum_{a=1,2,4,5,3z} g_a \int_{-\infty}^{+\infty} \frac{d\omega}{2\pi} \int \frac{d^3\mathbf{k}}{(2\pi)^3} \text{Tr} [\Gamma_X G_0(i\omega, \mathbf{k}) \Gamma_a G_0(i\omega, \mathbf{k})]. \quad (\text{C2})$$

The one-loop correction for the source term Δ_X resulting from Fig. 7(b) can be written as

$$W_{\Delta_X}^{(2)} = 2\Delta_X \sum_{a=1,2,4,5,3z} g_a \int_{-\infty}^{+\infty} \frac{d\omega}{2\pi} \int' \frac{d^3\mathbf{k}}{(2\pi)^3} (\bar{\Psi}\Gamma_a G_0(i\omega, \mathbf{k})\Gamma_X G_0(i\omega, \mathbf{k})\Gamma_a\Psi). \quad (\text{C3})$$

Substituting Eq. (B1) into Eq. (C2), we find

$$W_{\Delta_1}^{(1)} = 0, \quad (\text{C4})$$

$$W_{\Delta_2}^{(1)} = \Delta_2 g_2 \frac{2\Lambda^{\frac{3}{2}}}{\pi^2 v^2 \sqrt{A}} \ell (\bar{\Psi}\Psi), \quad (\text{C5})$$

$$W_{\Delta_{3\perp}}^{(1)} = 0, \quad (\text{C6})$$

$$W_{\Delta_{3z}}^{(1)} = \Delta_{3z} g_{3z} \frac{2\Lambda^{\frac{3}{2}}}{5\pi^2 v^2 \sqrt{A}} \ell (\bar{\Psi}\gamma_0\gamma_3\Psi), \quad (\text{C7})$$

$$W_{\Delta_4}^{(1)} = 0, \quad (\text{C8})$$

$$W_{\Delta_5}^{(1)} = \Delta_5 g_5 \frac{2\Lambda^{\frac{3}{2}}}{\pi^2 v^2 \sqrt{A}} \ell (\bar{\Psi}i\gamma_5\Psi), \quad (\text{C9})$$

$$W_{\Delta_{6\perp}}^{(1)} = 0, \quad (\text{C10})$$

$$W_{\Delta_{6z}}^{(1)} = 0, \quad (\text{C11})$$

$$W_{\Delta_{7\perp}}^{(1)} = 0, \quad (\text{C12})$$

$$W_{\Delta_{7z}}^{(1)} = 0, \quad (\text{C13})$$

$$W_{\Delta_{8\perp}}^{(1)} = 0, \quad (\text{C14})$$

$$W_{\Delta_{8z}}^{(1)} = 0. \quad (\text{C15})$$

Substituting Eq. (B1) into Eq. (C3), we obtain

$$W_{\Delta_1}^{(2)} = 0, \quad (\text{C16})$$

$$W_{\Delta_2}^{(2)} = \frac{1}{2}\Delta_2 (-g_1 - g_2 + g_4 + g_5 + g_{3z}) \frac{\Lambda^{\frac{3}{2}}}{\pi^2 v^2 \sqrt{A}} \ell (\bar{\Psi}\Psi), \quad (\text{C17})$$

$$W_{\Delta_{3\perp}}^{(2)} = \Delta_{3\perp} (-g_1 + g_2 + g_4 - g_5 + g_{3z}) \frac{\Lambda^{\frac{3}{2}}}{5\pi^2 v^2 \sqrt{A}} \ell \sum_{j=1}^2 (\bar{\Psi}\gamma_0\gamma_j\Psi), \quad (\text{C18})$$

$$W_{\Delta_{3z}}^{(2)} = \Delta_{3z} (-g_1 + g_2 + g_4 - g_5 - g_{3z}) \frac{\Lambda^{\frac{3}{2}}}{10\pi^2 v^2 \sqrt{A}} \ell (\bar{\Psi}\gamma_0\gamma_3\Psi), \quad (\text{C19})$$

$$W_{\Delta_4}^{(2)} = 0, \quad (\text{C20})$$

$$W_{\Delta_5}^{(2)} = \Delta_5 (-g_1 + g_2 + g_4 - g_5 - g_{3z}) \frac{\Lambda^{\frac{3}{2}}}{2\pi^2 v^2 \sqrt{A}} \ell (\bar{\Psi}i\gamma_5\Psi), \quad (\text{C21})$$

$$W_{\Delta_{6\perp}}^{(2)} = \Delta_{6\perp} (-g_1 - g_2 + g_4 + g_5 - g_{3z}) \frac{\Lambda^{\frac{3}{2}}}{5\pi^2 v^2 \sqrt{A}} \ell \sum_{\langle\langle lk \rangle\rangle} (\bar{\Psi}i\gamma_l\gamma_k\Psi), \quad (\text{C22})$$

$$W_{\Delta_{6z}}^{(2)} = \Delta_{6z} (-g_1 - g_2 + g_4 + g_5 + g_{3z}) \frac{\Lambda^{\frac{3}{2}}}{10\pi^2 v^2 \sqrt{A}} \ell (\bar{\Psi}i\gamma_1\gamma_2\Psi), \quad (\text{C23})$$

$$W_{\Delta_{7\perp}}^{(2)} = \Delta_{7\perp} (-g_1 - g_2 - g_4 - g_5 + g_{3z}) \frac{3\Lambda^{\frac{3}{2}}}{10\pi^2 v^2 \sqrt{A}} \ell \sum_{j=1}^2 (\bar{\Psi}i\gamma_5\gamma_j\Psi), \quad (\text{C24})$$

$$W_{\Delta_{7z}}^{(2)} = -\Delta_{7z} (g_1 + g_2 + g_4 + g_5 + g_{3z}) \frac{2\Lambda^{\frac{3}{2}}}{5\pi^2 v^2 \sqrt{A}} \ell (\bar{\Psi}i\gamma_5\gamma_3\Psi), \quad (\text{C25})$$

$$W_{\Delta_{8\perp}}^{(2)} = \Delta_{8\perp} (-g_1 + g_2 - g_4 + g_5 - g_{3z}) \frac{3\Lambda^{\frac{3}{2}}}{10\pi^2 v^2 \sqrt{A}} \ell \sum_{j=1}^2 (\bar{\Psi}i\gamma_j\Psi), \quad (\text{C26})$$

$$W_{\Delta_{8z}}^{(2)} = \Delta_{8z} (-g_1 + g_2 - g_4 + g_5 + g_{3z}) \frac{2\Lambda^{\frac{3}{2}}}{5\pi^2 v^2 \sqrt{A}} \ell (\bar{\Psi} i \gamma_3 \Psi). \quad (\text{C27})$$

From

$$W_{\Delta_X} = W_{\Delta_X}^{(1)} + W_{\Delta_X}^{(2)}, \quad (\text{C28})$$

we arrive

$$W_{\Delta_X} = \delta\Delta_X (\bar{\Psi} \Gamma_X \Psi). \quad (\text{C29})$$

The parameters $\delta\Delta_X$ are given by

$$\delta\Delta_1 = 0, \quad (\text{C30})$$

$$\delta\Delta_2 = \Delta_2 (-g_1 + 3g_2 + g_4 + g_5 + g_{3z}) \frac{\Lambda^{\frac{3}{2}}}{2\pi^2 v^2 \sqrt{A}} \ell, \quad (\text{C31})$$

$$\delta\Delta_{3\perp} = \Delta_{3\perp} (-g_1 + g_2 + g_4 - g_5 + g_{3z}) \frac{\Lambda^{\frac{3}{2}}}{5\pi^2 v^2 \sqrt{A}} \ell, \quad (\text{C32})$$

$$\delta\Delta_{3z} = \Delta_{3z} (-g_1 + g_2 + g_4 - g_5 + 3g_{3z}) \frac{\Lambda^{\frac{3}{2}}}{10\pi^2 v^2 \sqrt{A}} \ell, \quad (\text{C33})$$

$$\delta\Delta_4 = 0, \quad (\text{C34})$$

$$\delta\Delta_5 = \Delta_5 (-g_1 + g_2 + g_4 + 3g_5 - g_{3z}) \frac{\Lambda^{\frac{3}{2}}}{2\pi^2 v^2 \sqrt{A}} \ell, \quad (\text{C35})$$

$$\delta\Delta_{6\perp} = \Delta_{6\perp} (-g_1 - g_2 + g_4 + g_5 - g_{3z}) \frac{\Lambda^{\frac{3}{2}}}{5\pi^2 v^2 \sqrt{A}} \ell, \quad (\text{C36})$$

$$\delta\Delta_{6z} = \Delta_{6z} (-g_1 - g_2 + g_4 + g_5 + g_{3z}) \frac{\Lambda^{\frac{3}{2}}}{10\pi^2 v^2 \sqrt{A}} \ell, \quad (\text{C37})$$

$$\delta\Delta_{7\perp} = \Delta_{7\perp} (-g_1 - g_2 - g_4 - g_5 + g_{3z}) \frac{3\Lambda^{\frac{3}{2}}}{10\pi^2 v^2 \sqrt{A}} \ell, \quad (\text{C38})$$

$$\delta\Delta_{7z} = \Delta_{7z} (-g_1 - g_2 - g_4 - g_5 - g_{3z}) \frac{2\Lambda^{\frac{3}{2}}}{5\pi^2 v^2 \sqrt{A}} \ell, \quad (\text{C39})$$

$$\delta\Delta_{8\perp} = \Delta_{8\perp} (-g_1 + g_2 - g_4 + g_5 - g_{3z}) \frac{3\Lambda^{\frac{3}{2}}}{10\pi^2 v^2 \sqrt{A}} \ell, \quad (\text{C40})$$

$$\delta\Delta_{8z} = \Delta_{8z} (-g_1 + g_2 - g_4 + g_5 + g_{3z}) \frac{2\Lambda^{\frac{3}{2}}}{5\pi^2 v^2 \sqrt{A}} \ell. \quad (\text{C41})$$

2. One-loop order correction for source terms in particle-particle channel

In particle-particle channel, to one-loop order, there is one Feynman diagram as shown in Fig. 7(c) resulting in the correction to source terms. The correction can be expressed as

$$W_{\Delta_Y} = 2\Delta_Y \sum_{a=1,2,4,5,3z} g_a \int_{-\infty}^{+\infty} \frac{d\omega}{2\pi} \int' \frac{d^3\mathbf{k}}{(2\pi)^3} (\Psi^\dagger \Gamma_a^T G_0^T(i\omega, \mathbf{k}) \Gamma_Y G_0(-i\omega, -\mathbf{k}) \Gamma_a \Psi^*), \quad (\text{C42})$$

where T represents transposition. Substituting Eq. (B1) into Eq. (C42), we get

$$W_{\Delta_Y} = \delta\Delta_Y (\Psi^\dagger \Gamma_Y \Psi), \quad (\text{C43})$$

where

$$\delta\Delta_S = \Delta_S (g_1 - g_2 + g_4 + g_5 - g_{3z}) \frac{2\Lambda^{\frac{3}{2}}}{5\pi^2 v^2 \sqrt{A}} \ell, \quad (\text{C44})$$

$$\delta\Delta_{op} = \Delta_{op} (g_1 + g_2 + g_4 - g_5 + g_{3z}) \frac{2\Lambda^{\frac{3}{2}}}{5\pi^2 v^2 \sqrt{A}} \ell, \quad (\text{C45})$$

$$\delta\Delta_{V,1} = \Delta_{V,1} (g_1 + g_2 - g_4 + g_5 + g_{3z}) \frac{\Lambda^{\frac{3}{2}}}{5\pi^2 v^2 \sqrt{A}} \ell, \quad (\text{C46})$$

$$\delta\Delta_{V,2} = \Delta_{V,2} (g_1 + g_2 - g_4 + g_5 + g_{3z}) \frac{\Lambda^{\frac{3}{2}}}{5\pi^2 v^2 \sqrt{A}} \ell, \quad (\text{C47})$$

$$\delta\Delta_{V,3} = \Delta_{V,3} (g_1 + g_2 - g_4 + g_5 - g_{3z}) \frac{\Lambda^{\frac{3}{2}}}{2\pi^2 v^2 \sqrt{A}} \ell, \quad (\text{C48})$$

$$\delta\Delta_{V,0} = \Delta_{V,0} (g_1 - g_2 - g_4 - g_5 + g_{3z}) \frac{\Lambda^{\frac{3}{2}}}{20\pi^2 v^2 \sqrt{A}} \ell. \quad (\text{C49})$$

3. Derivation of the RG equations for source terms

In particle-hole channel, the bare action for the source terms is

$$S_s = \Delta_X \int \frac{d\omega}{2\pi} \frac{d^3\mathbf{k}}{(2\pi)^3} \bar{\Psi}(\omega, \mathbf{k}) \Gamma_X \Psi(\omega, \mathbf{k}). \quad (\text{C50})$$

Considering the one-loop order corrections, we obtain

$$S_s = (\Delta_X + \delta\Delta_X) \int \frac{d\omega}{2\pi} \frac{d^3\mathbf{k}}{(2\pi)^3} \bar{\Psi}(\omega, \mathbf{k}) \Gamma_X \Psi(\omega, \mathbf{k}). \quad (\text{C51})$$

Using the transformations Eqs. (B67)-B70) and (B73), we can get

$$\begin{aligned} S_s &= (\Delta_X + \delta\Delta_X) e^\ell \int \frac{d\omega'}{2\pi} \frac{d^3\mathbf{k}'}{(2\pi)^3} \bar{\Psi}'(\omega', \mathbf{k}') \Gamma_X \Psi'(\omega', \mathbf{k}') \\ &\approx (\Delta_X + \Delta_X \ell + \delta\Delta_X) \int \frac{d\omega'}{2\pi} \frac{d^3\mathbf{k}'}{(2\pi)^3} \bar{\Psi}'(\omega', \mathbf{k}') \Gamma_X \Psi'(\omega', \mathbf{k}'). \end{aligned} \quad (\text{C52})$$

Let

$$\Delta'_X = \Delta_X + \Delta_X \ell + \delta\Delta_X, \quad (\text{C53})$$

the action can be further written as

$$S_s = \Delta'_X \int \frac{d\omega'}{2\pi} \frac{d^3\mathbf{k}'}{(2\pi)^3} \bar{\Psi}'(\omega', \mathbf{k}') \Gamma_X \Psi'(\omega', \mathbf{k}'), \quad (\text{C54})$$

which recovers the form of the original action. We can easily find that the RG equation for Δ_X is

$$\frac{d\Delta_X}{d\ell} = \Delta_X + \frac{d\delta\Delta_X}{d\ell}. \quad (\text{C55})$$

Performing similar rescaling transformations, we can get the RG equation for source terms in particle-particle channel

$$\frac{d\Delta_Y}{d\ell} = \Delta_Y + \frac{d\delta\Delta_Y}{d\ell}. \quad (\text{C56})$$

Substituting Eqs. (C30)-(C41) into Eq. (C55), and substituting Eqs. (C44)-(C49) into Eq. (C56), we get the RG equations

$$\bar{\beta}_1 = 0, \quad (C57)$$

$$\bar{\beta}_2 = \frac{1}{2}(-g_1 + 3g_2 + g_4 + g_5 + g_{3z}), \quad (C58)$$

$$\bar{\beta}_{3\perp} = \frac{1}{5}(-g_1 + g_2 + g_4 - g_5 + g_{3z}), \quad (C59)$$

$$\bar{\beta}_{3z} = \frac{1}{10}(-g_1 + g_2 + g_4 - g_5), \quad (C60)$$

$$\bar{\beta}_4 = 0, \quad (C61)$$

$$\bar{\beta}_5 = \frac{1}{2}(-g_1 + g_2 + g_4 + 3g_5 - g_{3z}), \quad (C62)$$

$$\bar{\beta}_{6\perp} = \frac{1}{5}(-g_1 - g_2 + g_4 + g_5 - g_{3z}), \quad (C63)$$

$$\bar{\beta}_{6z} = \frac{1}{10}(-g_1 - g_2 + g_4 + g_5 + g_{3z}), \quad (C64)$$

$$\bar{\beta}_{7\perp} = \frac{3}{10}(-g_1 - g_2 - g_4 - g_5 + g_{3z}), \quad (C65)$$

$$\bar{\beta}_{7z} = \frac{2}{5}(-g_1 - g_2 - g_4 - g_5 - g_{3z}), \quad (C66)$$

$$\bar{\beta}_{8\perp} = \frac{3}{10}(-g_1 + g_2 - g_4 + g_5 - g_{3z}), \quad (C67)$$

$$\bar{\beta}_{8z} = \frac{2}{5}(-g_1 + g_2 - g_4 + g_5 + g_{3z}), \quad (C68)$$

$$\bar{\beta}_S = \frac{2}{5}(g_1 - g_2 + g_4 + g_5 - g_{3z}), \quad (C69)$$

$$\bar{\beta}_{op} = \frac{2}{5}(g_1 + g_2 + g_4 - g_5 + g_{3z}), \quad (C70)$$

$$\bar{\beta}_{V,1} = \frac{1}{5}(g_1 + g_2 - g_4 + g_5 + g_{3z}), \quad (C71)$$

$$\bar{\beta}_{V,2} = \frac{1}{5}(g_1 + g_2 - g_4 + g_5 + g_{3z}), \quad (C72)$$

$$\bar{\beta}_{V,3} = \frac{1}{2}(g_1 + g_2 - g_4 + g_5 - g_{3z}), \quad (C73)$$

$$\bar{\beta}_{V,0} = \frac{1}{20}(g_1 - g_2 - g_4 - g_5 + g_{3z}), \quad (C74)$$

where

$$\bar{\beta}_{X,Y} = \frac{d \ln(\Delta_{X,Y})}{d\ell} - 1. \quad (C75)$$

For convenience, we show the physical meaning of different order parameters and corresponding fermion bilinear in Table II

Appendix D: Numerical Results

1. Fixed points and their properties

Solving the RG equations for g_a as shown in Eqs. (B80)-(B84), we obtained the real roots as following

$$\text{FP0 : } (g_1^*, g_2^*, g_4^*, g_5^*, g_{3z}^*) = (0, 0, 0, 0, 0) \quad (D1)$$

$$\text{FP1 : } (g_1^*, g_2^*, g_4^*, g_5^*, g_{3z}^*) = (0.152019, 1.25444, 0.459247, -0.561711, 0.0551435), \quad (D2)$$

$$\text{FP2 : } (g_1^*, g_2^*, g_4^*, g_5^*, g_{3z}^*) = (0.140905, -0.585585, 0.418385, 1.34668, 0.06996), \quad (D3)$$

$$\text{FP3 : } (g_1^*, g_2^*, g_4^*, g_5^*, g_{3z}^*) = (-0.100015, 0.575751, -0.61003, 0.775675, 0.199924), \quad (D4)$$

TABLE II: Physical meaning of different order parameters and the corresponding fermion bilinears.

Order Parameter	Fermion Bilinear	Physical meaning
Δ_1	$\bar{\Psi}\gamma_0\Psi$	chemical potential
Δ_2	$\bar{\Psi}\Psi$	scalar mass
$\Delta_{3\perp}$	$\sum_{j=1,2} \bar{\Psi}\gamma_0\gamma_j\Psi$	spin-orbit coupling within xy plane
Δ_{3z}	$\bar{\Psi}\gamma_0\gamma_3\Psi$	spin-orbit coupling along z axis
Δ_4	$\bar{\Psi}\gamma_0\gamma_5\Psi$	axial chemical potential
Δ_5	$\bar{\Psi}i\gamma_5\Psi$	pseudoscalar mass
$\Delta_{6\perp}$	$\bar{\Psi}(i\gamma_2\gamma_3 + \gamma_3\gamma_1)\Psi$	magnetization within xy plane
Δ_{6z}	$\bar{\Psi}i\gamma_1\gamma_2\Psi$	magnetization along z axis
$\Delta_{7\perp}$	$\sum_{j=1,2} \bar{\Psi}i\gamma_5\gamma_j\Psi$	axial magnetization within xy plane
Δ_{7z}	$\bar{\Psi}i\gamma_5\gamma_3\Psi$	axial magnetization along z axis
$\Delta_{8\perp}$	$\sum_{j=1,2} \bar{\Psi}i\gamma_j\Psi$	current within xy plane
Δ_{8z}	$\bar{\Psi}i\gamma_3\Psi$	current along z axis
Δ_S	$\Psi^\dagger i\gamma_0\gamma_5\gamma_2\Psi^*$	s -wave paring
Δ_{op}	$\Psi^\dagger i\gamma_0\gamma_2\Psi^*$	odd-parity pairing
$\Delta_{V,1}$	$\Psi^\dagger\gamma_3\Psi^*$	vector pairing along x axis
$\Delta_{V,2}$	$\Psi^\dagger i\gamma_0\gamma_5\Psi^*$	vector pairing along y axis
$\Delta_{V,3}$	$\Psi^\dagger\gamma_1\Psi^*$	vector pairing along z axis
$\Delta_{V,0}$	$\Psi^\dagger i\gamma_0\gamma_1\gamma_3\Psi^*$	temporal vector paring

$$\text{FP4 : } (g_1^*, g_2^*, g_4^*, g_5^*, g_{3z}^*) = (-2.33263, 0., -0.610178, -1.72246, -1.72246), \quad (\text{D5})$$

$$\text{FP5 : } (g_1^*, g_2^*, g_4^*, g_5^*, g_{3z}^*) = (0.126936, -0.463077, -0.854005, 0.769245, 1.23232), \quad (\text{D6})$$

$$\text{FP6 : } (g_1^*, g_2^*, g_4^*, g_5^*, g_{3z}^*) = (0.0860014, 1.37623, 0.236822, -0.304132, 0.0941005), \quad (\text{D7})$$

$$\text{FP7 : } (g_1^*, g_2^*, g_4^*, g_5^*, g_{3z}^*) = (0.103947, -0.465334, 0.29293, 1.43995, 0.0944817), \quad (\text{D8})$$

$$\text{FP8 : } (g_1^*, g_2^*, g_4^*, g_5^*, g_{3z}^*) = (-3.33745, -1.22097, -1.28072, -1.32395, -0.102973), \quad (\text{D9})$$

$$\text{FP9 : } (g_1^*, g_2^*, g_4^*, g_5^*, g_{3z}^*) = (-2.68181, 1.06255, -1.97657, -1.35604, -2.41859), \quad (\text{D10})$$

$$\text{FP10 : } (g_1^*, g_2^*, g_4^*, g_5^*, g_{3z}^*) = (0, 0, -1.25, 1.25, 1.25), \quad (\text{D11})$$

$$\text{FP11 : } (g_1^*, g_2^*, g_4^*, g_5^*, g_{3z}^*) = (-5.16737, 0, -4.38982, -0.777544, -0.777544), \quad (\text{D12})$$

FP0 is the trivial Gauss fixed point. FP1-FP11 are non-trivial fixed points.

Expanding the RG equations (B80)-(B84) in the vicinity of a fixed point $(g_1^*, g_2^*, g_4^*, g_5^*, g_{3z}^*)$, we find that

$$\frac{dG}{d\ell} = MG, \quad (\text{D13})$$

where

$$G = \begin{pmatrix} \delta g_1 \\ \delta g_2 \\ \delta g_4 \\ \delta g_5 \\ \delta g_{3z} \end{pmatrix}, \quad (\text{D14})$$

with $\delta g_a = g_a - g_a^*$. The matrix M is given by

$$M = \begin{pmatrix} M_{11} & M_{12} & M_{13} & M_{14} & M_{15} \\ M_{21} & M_{22} & M_{23} & M_{24} & M_{25} \\ M_{31} & M_{32} & M_{33} & M_{34} & M_{35} \\ M_{41} & M_{42} & M_{43} & M_{44} & M_{45} \\ M_{51} & M_{52} & M_{53} & M_{54} & M_{55} \end{pmatrix}, \quad (\text{D15})$$

where

$$M_{11} = -\left(\frac{3}{2} + \frac{2}{5}g_2^* + \frac{1}{5}g_4^* + \frac{2}{5}g_5^*\right), \quad (\text{D16})$$

$$M_{12} = -\frac{2}{5}(g_1^* + g_5^*), \quad (\text{D17})$$

$$M_{13} = -\left(\frac{1}{5}g_1^* + \frac{2}{5}g_{3z}^*\right), \quad (\text{D18})$$

$$M_{14} = -\frac{2}{5}(g_1^* + g_2^* + g_{3z}^*), \quad (\text{D19})$$

$$M_{15} = -\frac{2}{5}(g_4^* + g_5^*), \quad (\text{D20})$$

$$M_{21} = -\frac{3}{5}g_2^* - \frac{2}{5}g_5^*, \quad (\text{D21})$$

$$M_{22} = -\frac{3}{2} + 2g_2^* - \frac{3}{5}g_1^* + \frac{4}{5}g_4^* + \frac{3}{5}g_5^* + g_{3z}^*, \quad (\text{D22})$$

$$M_{23} = \frac{4}{5}g_2^* - g_5^* + \frac{7}{5}g_{3z}^*, \quad (\text{D23})$$

$$M_{24} = \frac{3}{5}g_2^* - \frac{2}{5}g_1^* - g_4^* + \frac{2}{5}g_{3z}^*, \quad (\text{D24})$$

$$M_{25} = g_2^* + \frac{7}{5}g_4^* + \frac{2}{5}g_5^*, \quad (\text{D25})$$

$$M_{31} = -\frac{2}{5}g_1^* + \frac{2}{5}g_2^* + \frac{2}{5}g_5^*, \quad (\text{D26})$$

$$M_{32} = -\frac{2}{5}g_2^* + \frac{2}{5}g_1^* - \frac{7}{5}g_5^* + g_{3z}^*, \quad (\text{D27})$$

$$M_{33} = -\frac{3}{2} - \frac{2}{5}g_4^* + \frac{2}{5}g_{3z}^*, \quad (\text{D28})$$

$$M_{34} = -\frac{2}{5}g_5^* + \frac{2}{5}g_1^* - \frac{7}{5}g_2^* - \frac{1}{5}g_{3z}^*, \quad (\text{D29})$$

$$M_{35} = -\frac{2}{5}g_{3z}^* + \frac{2}{5}g_4^* + g_2^* - \frac{1}{5}g_5^*, \quad (\text{D30})$$

$$M_{41} = \frac{2}{5}g_1^* - g_5^* - \frac{4}{5}g_2^* - \frac{1}{5}g_4^*, \quad (\text{D31})$$

$$M_{42} = \frac{2}{5}g_2^* + g_5^* - \frac{4}{5}g_1^* - \frac{4}{5}g_4^* - g_{3z}^*, \quad (\text{D32})$$

$$M_{43} = \frac{2}{5}g_4^* + g_5^* - \frac{1}{5}g_1^* - \frac{4}{5}g_2^* - \frac{8}{5}g_{3z}^*, \quad (\text{D33})$$

$$M_{44} = -\frac{3}{2} + \frac{12}{5}g_5^* - g_1^* + g_2^* + g_4^* - g_{3z}^*, \quad (\text{D34})$$

$$M_{45} = \frac{2}{5}g_{3z}^* - g_5^* - g_2^* - \frac{8}{5}g_4^*, \quad (\text{D35})$$

$$M_{51} = \frac{2}{5}g_1^* - \frac{1}{5}g_{3z}^* - \frac{2}{5}g_2^* - \frac{1}{5}g_4^* - \frac{2}{5}g_5^*, \quad (\text{D36})$$

$$M_{52} = \frac{2}{5}g_2^* - \frac{4}{5}g_{3z}^* - \frac{2}{5}g_1^* + \frac{1}{5}g_4^* + \frac{2}{5}g_5^*, \quad (\text{D37})$$

$$M_{53} = \frac{2}{5}g_4^* - \frac{6}{5}g_{3z}^* - \frac{1}{5}g_1^* + \frac{1}{5}g_2^* + \frac{1}{5}g_5^*, \quad (\text{D38})$$

$$M_{54} = \frac{2}{5}g_5^* - \frac{3}{5}g_{3z}^* - \frac{2}{5}g_1^* + \frac{2}{5}g_2^* + \frac{1}{5}g_4^*, \quad (\text{D39})$$

$$M_{55} = -\frac{3}{2} + \frac{4}{5}g_{3z}^* - \frac{1}{5}g_1^* - \frac{4}{5}g_2^* - \frac{6}{5}g_4^* - \frac{3}{5}g_5^*. \quad (\text{D40})$$

From eigenvalues of M at a fixed point $(g_1^*, g_2^*, g_4^*, g_5^*, g_{3z}^*)$, we can get the properties of the fixed point. A negative (positive) eigenvalue is corresponding to a stable (unstable) eigendirection [32, 34]. For quantum critical point (QCP), bicritical point (BCP), and tricritical point (TCP), there is/are one, two, and three unstable direction(s) respectively. For a QCP, the correlation length exponent is determined by the inverse of the corresponding positive eigenvalue.

Substituting the values of g_a^* at each fixed point into the expression M , we calculate the corresponding eigenvalues of M . The eigenvalues for the fixed points are shown in Table III. For FP0, the eigenvalues of M are always negative, thus FP0 is a stable fixed point. We can find that there is one positive eigenvalue for FP1, FP2, FP3, FP4, and FP5, and there are two positive eigenvalues for FP6, FP7, FP8, FP9, and FP10, and three positive eigenvalues for FP11. Thus, FP1, FP2, FP3, FP4, and FP5 are QCPs, FP6, FP7, FP8, FP9, and FP10 are BCPs, and FP11 is a TCP.

TABLE III: Eigenvalues of matrix M at different fixed points

FP0	FP1	FP2	FP3	FP4	FP5	FP6	FP7	FP8	FP9	FP10	FP11
-1.5	-3.12277	-3.05426	-2.11269	-4.19874	-2.50996	-2.98441	-2.99224	-5.70333	-5.29866	-2.25	-9.30126
-1.5	-2.7634	-2.48233	-1.42791	-2.79748	-2.05542	-2.77106	-2.49091	-3.26902	-3.36509	-2.25	-1.69424
-1.5	-1.77432	-1.76197	-1.26511	-2.46863	-1.41052	-1.80787	-1.77301	-1.46547	-1.38636	-1.47474	1.5
-1.5	-0.412398	-0.231803	-1.18664	-0.848268	-1.06884	0.390411	0.224733	1.5	1.5	0.974745	3.33999
-1.5	1.5	1.5	1.5	1.5	1.5	1.5	1.5	2.47601	2.17557	1.5	5.46863

It is easy to find that the correlation length exponent at the QCPs FP1, FP2, FP3, FP4 and FP5 all satisfy

$$\nu^{-1} = 1.5 \quad (\text{D41})$$

Substituting the values of g_a^* with $i = 1, 2, 4, 5, 3z$ into Eqs. (C57)-(C74), we can get values of $\bar{\beta}_{X,Y}$ for different $\Delta_{X,Y}$, which are shown in Tabel IV. For a QCP, the largest value of $\beta_{X,Y}$ is marked by the bold style. It represents that the fixed point is a QCP to the new state in which $\Delta_{X,Y}$ acquires finite value. FP1, FP2, FP4, and FP5 are corresponding to QCPs to a state in which Δ_2 , Δ_5 , Δ_{7z} and Δ_{8z} acquire finite value respectively. For FP3, it stands for a QCP to a state in which Δ_2 and Δ_5 become finite generally. This state represents an axionic insulator whose order parameter can be written as $\langle \bar{\Psi} (\cos(\theta) + i\gamma_5 \sin(\theta)) \Psi \rangle$ [33].

TABLE IV: $\beta_{X,Y}$ at different fixed points. The largest value at a QCP is marked by the bold style. Notice that FP1, FP2, FP3, FP4, FP5 are QCPs.

	FP1	FP2	FP3	FP4	FP5	FP6	FP7	FP8	FP9	FP10	FP11
β_1	0	0	0	0	0	0	0	0	0	0	0
β_2	1.78199	-0.0313166	1.09642	-0.861228	-0.184302	2.03474	0.163708	-1.51656	0.0591369	0.625	-0.388772
$\beta_{3\perp}$	0.435705	-0.316965	-0.102003	0.344491	-0.196188	0.385057	-0.324365	0.411346	0.141049	-0.25	0.155509
β_{3z}	0.212338	-0.165478	-0.070994	0.344491	-0.221326	0.183119	-0.171631	0.21597	0.312383	-0.25	0.155509
β_4	0	0	0	0	0	0	0	0	0	0	0
β_5	-0.0893033	1.83099	1.09642	-0.861228	-0.184302	0.260278	1.97451	-1.51656	0.0591369	0.625	-0.388772
$\beta_{6\perp}$	-0.312814	0.427957	-0.102003	0.344491	-0.196188	-0.324729	0.399958	0.411346	0.141049	-0.25	0.155509
β_{6z}	-0.145378	0.227971	-0.0110167	-0.172246	0.14837	-0.143544	0.218875	0.185078	-0.413193	0.125	-0.0777544
$\beta_{7\perp}$	-0.374656	-0.375128	-0.132437	0.882843	0.495967	-0.390247	-0.383104	2.11804	0.759982	0.375	2.86716
β_{7z}	-0.543656	-0.556138	-0.336522	2.55509	-0.324568	-0.59561	-0.586391	2.90643	2.94818	-0.5	4.44491
$\beta_{8\perp}$	0.00789679	0.0395537	0.558464	0.882843	-0.0597252	0.196553	0.144978	0.652867	2.03504	0.375	2.86716
β_{8z}	0.0546439	0.108706	0.904558	-0.20084	0.906224	0.337352	0.26889	0.788112	0.778521	1.5	3.20084
β_S	-0.504013	0.968638	-0.284018	-1.17712	-0.290828	-0.580657	0.883073	-1.84727	-1.86335	-0.5	-3.82288
β_{op}	0.993025	-0.521206	-0.284018	-1.17712	-0.290828	0.838916	-0.565572	-1.84727	-1.86335	-0.5	-3.82288
$\beta_{V,1}$	0.0881294	0.110715	0.412273	-1.03347	0.503886	0.203076	0.176024	-0.940925	-0.683464	0.75	-0.466527
$\beta_{V,2}$	0.0881294	0.110715	0.412273	-1.03347	0.503886	0.203076	0.176024	-0.940925	-0.683464	0.75	-0.466527
$\beta_{V,3}$	0.16518	0.206828	0.830758	-0.861228	0.027394	0.41359	0.345578	-2.24934	0.709928	0.625	-0.388772
$\beta_{V,0}$	-0.0472408	-0.0484308	-0.0320743	-0.0861228	0.0953547	-0.0564411	-0.053456	0.019261	-0.141517	0.0625	-0.0388772

[1] O. Vafek and A. Vishwanath, Dirac fermions in solids: From high- T_c cuprates and graphene to topological insu-

lators and Weyl semimetals, Annu. Rev. Condens. Matter

- Phys. **5**, 83 (2014).
- [2] T. O. Wehling, A. M. Black-Schaffer, and A. V. Balatsky, Dirac materials, *Adv. Phys.* **63**, 1 (2014).
- [3] B. Yan and C. Felser, Topological materials: Weyl semimetals, *Annu. Rev. Condens. Matter Phys.* **8**, 337 (2017).
- [4] M. Z. Hasan, S.-Y. Xu, I. Belopolski, and S.-M. Huang, Discovery of Weyl fermion semimetals and topological Fermi arc states, *Annu. Rev. Condens. Matter Phys.* **8**, 289 (2017).
- [5] N. P. Armitage, E. J. Mele, and A. Vishwanath, Weyl and Dirac semimetals in three-dimensional solids, *Rev. Mod. Phys.* **90**, 015001 (2018).
- [6] J. Kruthoff, J. de Boer, J. van Wezel, C. L. Kane, and R.-J. Slager, Topological classification of crystalline insulators through band structure combinatorics, *Phys. Rev. X* **7**, 041069 (2017).
- [7] F. Tang, H. C. Po, A. Vishwanath, and X. Wan, Comprehensive search for topological materials using symmetry indicators, *Nature* **566**, 486 (2019).
- [8] T. Zhang, Y. Jiang, Z. Song, H. Huang, Y. He, Z. Fang, H. Weng, and C. Fang, Catalogue of topological electronic materials, *Nature* **566**, 475 (2019).
- [9] M. G. Vergniory, L. Elcoro, C. Felser, N. Regnault, B. A. Bernevig, and Z. Wang, A complete catalogue of high-quality topological materials, *Nature* **566**, 480 (2019).
- [10] B. Lv, T. Qian, and H. Ding, Angle-resolved photoemission spectroscopy and its application to topological materials, *Nat. Rev. Phys.* **1**, 609 (2019).
- [11] G. Xu, H. Weng, Z. Wang, X. Dai, and Z. Fang, Chern semimetal and the quantized anomalous Hall effect in HgCr_2Se_4 , *Phys. Rev. Lett.* **107**, 186806 (2011).
- [12] C. Fang, M. J. Gilbert, X. Dai, and B. A. Bernevig, Multi-Weyl topological semimetals stabilized by point group symmetry, *Phys. Rev. Lett.* **108**, 266802 (2012).
- [13] P. Dietl, F. Piéchon, and G. Montambaux, *New magnetic field dependence of Landau levels in a graphenelike structure*, *Phys. Rev. Lett.* **100**, 236405 (2008).
- [14] B.-J. Yang and N. Nagaosa, Classification of stable three-dimensional Dirac semimetals with nontrivial topology, *Nat. Commun.* **5**, 4898 (2014).
- [15] B. Bradlyn, J. Cano, Z. Wang, M. G. Vergniory, R. J. Cava, and B. A. Bernevig, Beyond Dirac and Weyl fermions: Unconventional quasiparticles in conventional crystals, *Science* **353**, aaf5037 (2016).
- [16] P. Tang, Q. Zhou, and S.-C. Zhan, Multiple types of topological fermions in transition metal silicides, *Phys. Rev. Lett.* **119**, 206402 (2017).
- [17] T. Zhang, Z. Song, A. Alexandradinata, H. Weng, C. Fang, L. Lu, and Z. Fang, Double-Weyl phonons in transition-Metal monosilicides, *Phys. Rev. Lett.* **120**, 016401 (2018).
- [18] D. Takane, Z. Wang, S. Souma, K. Nakayama, T. Nakamura, H. Oinuma, Y. Nakata, H. Iwasawa, C. Cacho, T. Kim, K. Horiba, H. Kumigashira, T. Takahashi, Y. Ando, and T. Sato, Observation of chiral fermions with a large topological charge and associated Fermi-arc surface states in CoSi , *Phys. Rev. Lett.* **122**, 076402 (2019).
- [19] Z. Rao, H. Li, T. Zhang, S. Tian, C. Li, B. Fu, C. Tang, L. Wang, Z. Li, W. Fan, J. Li, Y. Huang, Z. Liu, Y. Long, C. Fang, H. Weng, Y. Shi, H. Lei, Y. Sun, T. Qian, and H. Ding, Observation of unconventional chiral fermions with long Fermi arcs in CoSi , *Nature* **567**, 496 (2019).
- [20] D. S. Sanchez, I. Belopolski, T. A. Cochran, X. Xu, J.-X. Yin, G. Chang, W. Xie, K. Manna, V. Süß, C.-Y. Huang, N. Alidoust, D. Multer, S. S. Zhang, N. Shumiya, X. Wang, G.-Q. Wang, T.-R. Chang, C. Felser, S.-Y. Xu, S. Jia, H. Lin, and M. Z. Hasan, Topological chiral crystals with helicoid-arc quantum states, *Nature* **567**, 500, (2019).
- [21] N. B. M. Schröter, D. Pei, M. G. Vergniory, Y. Sun, K. Manna, F. de Juan, J. A. Krieger, Süß, M. Schmidt, P. Dudin, B. Bradlyn, T. K. Kim, T. Schmitt, C. Cacho, C. Felser, V. N. Strocov, and Y. Chen, Chiral topological semimetal with multifold band crossings and long Fermi arcs, *Nat. Phys.* **15**, 759 (2019).
- [22] N. B. M. Schröter, S. Stolz, K. Manna, F. de Juan, M. G. Vergniory, J. A. Krieger, D. Pei, T. Schmitt, P. Dudin, T. K. Kim, C. Cacho, B. Bradlyn, H. Borrmann, M. Schmidt, R. Widmer, V. N. Strocov, and C. Felser, Observation and control of maximal Chern numbers in a chiral topological semimetal, *Science* **369**, 179 (2020).
- [23] V. N. Kotov, B. Uchoa, V. M. Pereira, F. Guinea, and A. H. Castro Neto, Electron-electron interactions in graphene: Current status and perspectives, *Rev. Mod. Phys.* **84**, 1067 (2012).
- [24] J.-R. Wang and G.-Z. Liu, Absence of dynamical gap generation in suspended graphene, *New J. Phys.* **14**, 043036 (2012).
- [25] J. Hofmann, E. Barnes, and S. Das Sarma, Why does graphene behave as a weakly interacting system?, *Phys. Rev. Lett.* **113**, 105502 (2014).
- [26] P. Goswami and S. Chakravarty, Quantum criticality between topological and band insulators in 3+1 dimensions, *Phys. Rev. Lett.* **107**, 196803 (2011).
- [27] P. Hosur, S. A. Parameswaran, and A. Vishwanath, Charge transport in Weyl semimetals, *Phys. Rev. Lett.* **108**, 046602 (2012).
- [28] H.-K. Tang, J. N. Leaw, J. N. B. Rodrigues, I. F. Herbut, P. Sengupta, F. F. Assaad, and S. Adam, The role of electron-electron interactions in two-dimensional Dirac fermions, *Science* **361**, 570 (2018).
- [29] J. N. Leaw, H.-K. Tang, M. Trushin, F. F. Assaad, and S. Adam, Universal Fermi-surface anisotropy renormalization for interacting Dirac fermions with long-range interactions, *Proc. Natl. Acad. Sci. U.S.A.* **116**, 24631 (2019).
- [30] I. F. Herbut, Interactions and phase transitions on graphene's honeycomb lattice, *Phys. Rev. Lett.* **97**, 146401 (2006).
- [31] I. F. Herbut, V. Juričić, and B. Roy, Theory of interacting electrons on the honeycomb lattice, *Phys. Rev. B* **79**, 085116 (2009).
- [32] J. Maciejko and R. Nandkishore, Weyl semimetals with short-range interactions, *Phys. Rev. B* **90**, 035126 (2014).
- [33] B. Roy and S. Das Sarma, Quantum phases of interacting electrons in three-dimensional dirty Dirac semimetals, *Phys. Rev. B* **94**, 115137 (2016).
- [34] A. L. Szabó and B. Roy, Emergent chiral symmetry in a three-dimensional interacting Dirac liquid, *J. High Energy Phys.* **01** (2021) 004.
- [35] E.-G. Moon, C. Xu, Y. B. Kim, and L. Balents, Non-Fermi-liquid and topological states with strong spin-orbit coupling, *Phys. Rev. Lett.* **111**, 206401 (2013).
- [36] I. F. Herbut and L. Janssen, Topological Mott insulator in three-dimensional systems with quadratic band touching, *Phys. Rev. Lett.* **113**, 106401 (2014).
- [37] B.-J. Yang, E.-G. Moon, H. Isobe, and N. Nagaosa, Quantum criticality of topological phase transitions in

- three-dimensional interacting electronic systems, *Nat. Phys.* **10**, 774 (2014).
- [38] A. A. Abrikosov, Gapless state of bismuth-type semimetals, *J. Low. Temp. Phys.* **8**, 315 (1972).
- [39] H. Isobe, B.-J. Yang, A. Chubukov, J. Schmalian, and N. Nagaosa, Emergent non-Fermi-liquid at the quantum critical point of a topological phase transition in two dimensions, *Phys. Rev. Lett.* **116**, 076803 (2016).
- [40] G. Y. Cho and E.-G. Moon, Novel quantum criticality in two dimensional topological phase transitions, *Sci. Rep.* **6**, 19198 (2016).
- [41] J.-R. Wang, G.-Z. Liu, and C.-J. Zhang, Excitonic pairing and insulating transition in two-dimensional semi-Dirac semimetals, *Phys. Rev. B* **95**, 075129 (2017).
- [42] H.-H. Lai, Correlation effects in double-Weyl semimetals, *Phys. Rev. B* **91**, 235131 (2015).
- [43] S.-K. Jian and H. Yao, Correlated double-Weyl semimetals with Coulomb interactions: Possible applications to HgCr_2Se_4 and SrSi_2 , *Phys. Rev. B* **92**, 045121 (2015).
- [44] J.-R. Wang, G.-Z. Liu, and C.-J. Zhang, Quantum phase transition and unusual critical behavior in multi-Weyl semimetals, *Phys. Rev. B* **96**, 165142 (2017).
- [45] S.-X. Zhang, S.-K. Jian, and H. Yao, Correlated triple-Weyl semimetals with Coulomb interactions, *Phys. Rev. B* **96**, 241111(R) (2017).
- [46] J.-R. Wang, G.-Z. Liu, and C.-J. Zhang, Breakdown of Fermi liquid theory in topological multi-Weyl semimetals, *Phys. Rev. B* **98**, 205113 (2018).
- [47] J.-R. Wang, G.-Z. Liu, and C.-J. Zhang, Topological quantum critical point in a triple-Weyl semimetal: Non-Fermi-liquid behavior and instabilities, *Phys. Rev. B* **99**, 195119 (2019).
- [48] S. Han, C. Lee, E.-G. Moon, and H. Min, Emergent anisotropic non-Fermi liquid at a topological phase transition in three dimensions, *Phys. Rev. Lett.* **122**, 187601 (2019).
- [49] S.-X. Zhang, S.-K. Jian, and H. Yao, Quantum criticality preempted by nematicity, arXiv:1809.10686.
- [50] B. Roy, M. P. Kennett, K. Yang, and V. Juričić, From birefringent electrons to a marginal or non-Fermi liquid of relativistic spin-1/2 fermions: An emergent superuniversality, *Phys. Rev. Lett.* **121**, 157602 (2018).
- [51] V. N. Kotov, B. Uchoa, and O. P. Sushov, Coulomb interactions and renormalization of semi-Dirac fermions near a topological Lifshitz transition, *Phys. Rev. B* **103**, 045403 (2021).
- [52] B. Roy, P. Goswami, and V. Juričić, Interacting Weyl fermions: Phases, phase transitions, and global phase diagram, *Phys. Rev. B* **95**, 201102(R) (2017).
- [53] B. Roy and M. S. Foster, Quantum multicriticality near the Dirac-semimetal to band-insulator critical point in two dimensions: A controlled ascent from one dimension, *Phys. Rev. X* **8**, 011049 (2018).
- [54] J. Wang, Role of four-fermion interaction and impurity in the states of two-dimensional semi-Dirac materials, *J. Phys.: Condens. Matter* **30**, 125401 (2018).
- [55] A. L. Szabó, R. Moessner, and B. Roy, Interacting spin-3/2 fermions in a Luttinger (semi)metal: competing phases and their selection in the global phase diagram, arXiv:1811.12415.
- [56] I. Boettcher, Interplay of topology and electron-electron interactions in Rarita-Schwinger-Weyl semimetals, *Phys. Rev. Lett.* **124**, 127602 (2020).
- [57] L. Savary, E.-G. Moon, and L. Balents, New type of quantum criticality in the pyrochlore iridates, *Phys. Rev. X* **4**, 041027 (2014).
- [58] M. D. Uryszek, E. Christou, A. Jaefari, F. Krüger, and B. Uchoa, Quantum criticality of semi-Dirac fermions in $2+1$ dimensions, *Phys. Rev. B* **100**, 155101 (2019).
- [59] S. Sur and B. Roy, Unifying interacting nodal semimetals: A new route to strong coupling, *Phys. Rev. Lett.* **123**, 207601 (2019).
- [60] M. D. Uryszek, F. Krüger, and E. Christou, Fermionic criticality of anisotropic nodal point semimetals away from the upper critical dimension: Exact exponents to leading order in $\frac{1}{N_f}$, *Phys. Rev. Research* **2**, 043265 (2020).
- [61] R. Shankar, Renormalization-group approach to interacting fermions, *Rev. Mod. Phys.* **66**, 129 (1994).
- [62] X. Yuan, C. Zhang, Y. Liu, A. Narayan, C. Song, S. Shen, X. Sui, J. Xu, H. Yu, Z. An, J. Zhao, S. Sanvito, H. Yan, and F. Xiu, Observation of quasi-two-dimensional Dirac fermions in ZrTe_5 , *NPG Asia Mater.* **8**, e325 (2016).
- [63] J. L. Zhang, C. Y. Guo, X. D. Zhu, L. Ma, G. L. Zheng, Y. Q. Wang, L. Pi, Y. Chen, H. Q. Yuan, and M. L. Tian, Disruption of the accidental Dirac semimetal state in ZrTe_5 under hydrostatic pressure, *Phys. Rev. Lett.* **118**, 206601 (2017).
- [64] E. Martino, I. Crassee, G. Eguchi, D. Santos-Cottin, R. D. Zhong, G. D. Gu, H. Berger, Z. Rukelj, Two-dimensional conical dispersion in ZrTe_5 evidenced by optical spectroscopy, *Phys. Rev. Lett.* **122**, 217402 (2019).
- [65] D. Santos-Cottin, M. Padleski, E. Martino, S. Ben David, F. Le Mardelé, F. Capitani, F. Borondics, M. D. Bachmann, C. Putzke, P. J. W. Moll, R. D. Zhong, G. D. Gu, H. Berger, M. Orlita, C. C. Homes, Z. Rukelj, and A. Akrap, Probing intraband excitations in ZrTe_5 : A high-pressure infrared and transport study, *Phys. Rev. B* **101**, 125205 (2020).
- [66] C. Zhang, J. Sun, F. Liu, A. Narayan, N. Li, X. Yuan, Y. Liu, J. Dai, Y. Long, Y. Uwatoko, J. Shen, S. Sanvito, W. Yang, J. Cheng, and F. Xiu, Evidence for pressure-induced node-pair annihilation in Cd_3As_2 , *Phys. Rev. B* **96**, 155205 (2017).